Dynamic measures of arterial stiffness in a rodent model

A Thesis Submitted to the
College of Graduate Studies and Research
in Partial Fulfillment of the Requirements
for the degree of Master of Science
in the Department of Veterinary Biomedical Sciences
University of Saskatchewan
Saskatoon

By
Kaylee Bohaychuk

Permission to Use

In presenting this thesis in partial fulfilment of the requirements for a Postgraduate degree from the University of Saskatchewan, I agree that the Libraries of this University may make it freely available for inspection. I further agree that permission for copying of this thesis in any manner, in whole or in part, for scholarly purposes may be granted by the professor or professors who supervised my thesis work or, in their absence, by the Head of the Department or the Dean of the College in which my thesis work was done. It is understood that any copying or publication or use of this thesis or parts thereof for financial gain shall not be allowed without my written permission. It is also understood that due recognition shall be given to me and to the University of Saskatchewan in any scholarly use which may be made of any material in my thesis.

Requests for permission to copy or to make other use of material in this thesis in whole or part should be addressed to:

Head of the Department of Veterinary Biomedical Sciences
Western College of Veterinary Medicine
University of Saskatchewan
52 Campus Drive
Saskatoon, Saskatchewan
Canada
S7N 5B4

Abstract

Cardiovascular disease is one of the leading causes of death in Canada. Arterial stiffness is an important factor in the pathogenesis of cardiovascular disease. Cardiac failure, hypertension, renal failure, and dementia have all been linked to arterial stiffness. The arterial system is designed to dampen the pulses of blood from the heart's left ventricle and distribute the blood forward as steady flow in the small vessels. The pulse-dampening ability of the arterial system is reduced with age when the elastic fibers in the arterial wall degrade and fracture. The arterial stiffening process can accelerate from deposition of minerals within the arterial wall, such as calcium, from the endothelial layer becoming compromised or from fibrosis secondary to inflammation or turbulence. Arterial stiffness can be assessed post-mortem by microscopic examination of the arterial wall. However, for use in dynamic experiments and for therapeutic intervention, several ante-mortem techniques have been developed: pulse wave velocity (PWV), pulse waveform analysis (PWA), wave separation analysis (WSA), and carotid ultrasonography. Rats are important models for cardiovascular disease, toxicology, and pharmacological studies because of their convenient size and short life cycle. However, PWA and WSA have not been shown to be valid approaches for studying arterial stiffness in rat peripheral arteries. In this thesis, dynamic in vivo methods for PWA and WSA in rat peripheral arteries were developed to provide accurate measures of arterial stiffness. Software specific to the rat vasculature, `PWanalyze` and `WSanalyze`, was developed to measure PWA and WSA parameters, respectively. A comparison of these PWA and WSA methods in rat peripheral arteries was performed by creating a range of arterial stiffnesses through acute and chronic experiments. Arterial stiffness was measured in the femoral artery by a novel PWA parameter, the minimum time derivative of blood pressure (dP/dt_{min}), as effectively as the established parameter the maximum time derivative of blood pressure (dP/dt_{max}). A new method of WSA in femoral arteries was developed. Backward wave amplitude measured in the aorta was shown to increase as arteries stiffened and decrease as arteries relaxed with acute vasoactive drug injections. These experiments showed that dP/dt_{min} and WSA are valid approaches to use when studying arterial stiffness in rats.

Acknowledgements

Thank you to my supervisor Dr. Lynn Weber for her support, funding, and guidance throughout this project. I would also like to thank the members of my committee, Dr. Ray Spiteri, Dr. Tanya Duke, and Dr. Ali Honoramooz, for supporting me and providing their scientific expertise. Thank you to the members of the cardiovascular toxicology lab for all of their assistance with experiments and friendly conversation. Thank you to the Merial Veterinary Scholars program, the Interprovincial Graduate Fellowship program, the western college of veterinary medicine, and the department of veterinary biomedical sciences for the funding and resources. Thank you to my husband, Adam Preuss, who always pushes me to do my best. Thank you to my parents, Sharon and Michael Bohaychuk, who always encouraged my curious brain. Special thank you to the professors of the Science 100 program at the University of Alberta, particularly Dr. Connie Varnhagen and Dr. Paul Lu, for taking the time to nuture my interest in research as an undergraduate student.

To Adam, Michael, and Sharon.

Contents

List of Tables

List of Figures

List of Abbreviations

AI_X	Augmentation Index
CA PSV	Carotid Artery Peak Systolic Velocity
cIMT	Carotid Intima-Media Thickness
DBP	Diastolic Blood Pressure
LOF	List of Figures
LOT	List of Tables
PP	Pulse Pressure
PWA	Pulse Waveform Analysis
PWV	Pulse Wave Velocity
SBP	Systolic Blood Pressure
TT	Transit-time
WSA	Wave Separation Analysis

Chapter 1

Introduction

1.1 Main Theme and Overall Structure

This thesis explores novel methods of measuring arterial stiffness in the rat and the cardiovascular hemodynamic principles supporting these methods. The motivation of this thesis is to address a major problem in preclinical biomedical science. There are many algorithms and indicators of arterial stiffness developed for humans that are not yet adapted to animal models, putting preclinical biomedical researchers at a major disadvantage because of a disconnect with human clinical end-points. The current methods of measuring arterial stiffness in rats are inadequate because they rely on multiple assumptions and their results are not easily reproducible between laboratories. To fill this gap in knowledge, this thesis presents two novel methods using intra-arterial blood pressure traces. Two independent studies were conducted. The first study investigates how the the rate at which blood pressure changes within an artery is related to arterial stiffness. The maximum rate of change of decreasing blood pressure, i.e., the minimum time derivative of blood pressure, dP/dt_{min}, was shown to be a novel indicator of arterial stiffness in addition to an established indicator of arterial stiffness, the maximum rate of change of increasing blood pressure, the maximum time derivative of blood pressure, dP/dt_{max}. The second study showed that wave separation analysis (WSA) could be used to assess wave reflections in the peripheral arteries. Wave reflections were demonstrated in the femoral artery with backward wave amplitude being a sensitive indicator of acute changes in arterial stiffness using vasoactive drug injections.

Chapter 2 is a data chapter introducing the novel dP/dt_{min} parameter for measuring acute and chronic changes in arterial stiffness. Chapter 3 provides a theoretical overview of the mathematical and physical principles that are the necessary background information for

wave separation analysis. Chapter 4 is a data chapter describing wave separation analysis in rats and the acute changes in wave reflections that occur in rats. Chapter 5 is a final discussion of the results, scientific contributions, and directions for future work.

1.2 Arterial Stiffness and Cardiovascular Disease

Epidemiological studies have demonstrated that arterial stiffness is associated with increased morbidity and mortality in humans [53, 96]. Cardiovascular disease accounts for a third of all deaths in the US and Canada [2, 27, 119]. Diseases caused by arterial stiffness include cardiac failure [67] and small vessel disease [96] of the kidney and brain leading to renal failure and dementia [10, 52, 82]. Arterial stiffness is a potential cause and consequence of hypertension [49]. Arterial stiffness causes hypertension through increased wave reflections as discussed in Section 1.3 [53]. Hypertension causes arterial stiffness by increased vascular smooth muscle cell hypertrophy and damage to the elastic components of the arterial wall [21]. Establishing a link between arterial stiffness and cardiovascular disease requires knowledge of the mechanical properties of arteries.

The central arteries have elastic properties; hence, arterial mechanics is based on the theory of elastic materials [88]. The ability of a solid material to return to its original shape after being deformed is defined as elasticity. The force used to stretch an elastic material over a unit distance is referred to as the *elastic modulus* [88]. The elastic modulus is a relative measure of the quantity of force required to stretch an elastic material. The elastic modulus in a longitudinal direction is called Young's modulus [88]:

$$E = \frac{\text{Longitudinal force per unit area}}{\text{Extension per unit length}}. \tag{1.1}$$

Stiff arteries have a large elastic modulus, whereas distensible arteries have a small elastic modulus. A stiff artery takes more force to stretch the same amount as a distensible artery. There are two major proteins which form the structure of the arterial wall: collagen and elastin. The collagen and elastin fibers partly determine the distensibility of the arterial wall along with endothelial cell function, vascular smooth muscle tone, and mineralization with calcium and phosphorus [139].

Predisposing factors that cause arterial stiffness include inflammation, hypertension, aging, and toxicity. Inflammation and hypertension both stimulate excessive collagen production, damage to elastin fibers, hypertrophy of vascular smooth muscle, and decreased normal elastin [139]. Age-related changes can also cause elastic structural protein damage, transferring stress on the arterial wall from elastin to collagen fibers [7, 55]. The collagen fibers have a higher elastic modulus than elastin fibers contributing to an overall stiffening of the arterial wall [91]. The degradation of elastin fibers from aging or inflammation is associated with increased calcification in the medial layer of the arterial wall [3, 79, 139]. Section 1.5 discusses arterial stiffness from toxicity relevant to the rodent model species used in this thesis.

A common example of arterial stiffening arises in elderly people, where the proximal aorta can be stiff from fracture of the elastin fibers [91]. Elastin has a half-life of decades; once it is damaged, the stress of each pulse is transferred to rigid collagenous components of the arterial wall [88]. The elastic modulus of the artery increases from elastin damage [88]. The force generated by blood ejection from the left ventricle dilates a stiff proximal aorta less than a distensible proximal aorta. Therefore, a stiff proximal aorta causes increased left ventricular load [91]. The heart compensates for increased load by increasing myocardial mass (hypertrophy), reducing capacity for filling with blood during diastole. Predisposition to myocardial ischemia and cardiac failure are consequences of increased metabolic demands of a hypertrophied, chronically loaded heart with reduced blood filling during diastole [91]. This reduced diastolic filling then causes the heart to stimulate its contractile force to increase heart rate to maintain cardiac output and creates a positive feedback mechanism leading to further myocardial hypertrophy and reduced blood filling during diastole [91]. Myocardial hypertrophy compromises the heart muscle perfusion during diastole, leading to myocardial ischemia [91]. Additionally, a stiff aorta is unable to dampen the pulsatile force from the heart, causing the pulsatile energy to propagate down the arterial system. This pulsatile energy damages the small vessels in vasodilated organs with vulnerable vascular beds (such as the kidney and brain) causing renal failure and dementia [10, 52, 82, 88].

1.3 Wave Reflection in the Arterial System

The arterial system can be thought of as a tree of distensible tubes, through which blood travels throughout the body. Blood movement throughout the body is characterized by three properties: pressure, flow, and resistance. Blood pressure is the force the blood exerts on the walls of an artery. Blood flow is the rate of movement of blood through an artery. Resistance is the opposition to blood flow through an artery.

Pressure waves and flow waves describe the manner in which blood pressure and blood flow pulse with each heart beat. The pressure and flow waves travel through the arterial system. At any variance in this system of arteries, such as a narrowing or branching of an artery, part of the wave travelling from the heart is transmitted forward past the variance and the remaining fraction is reflected backwards [88].

The closed-end tube model is a simplified model of the arterial system used to explain wave reflection, shown in Figure 1.1. The closed-end tube model of the arterial system is comprised of a long elastic tube filled with liquid, where liquid is pushed into the end of the tube, representing the heart ejecting blood. The other end is closed, representing the resistance to blood flow at a branch point or narrowing of the arterial tree [15, 88]. For each heart beat, the pressure generated against the tube edges that travels down the tube is called the forward pressure wave, P_f. Once the pressure wave reaches the closed end of the tube, it is reflected back in a pressure wave, P_b.

In 1956, Wetterer hypothesized that the pressure and flow waves measured in the arterial system were the sum of forward travelling waves from the heart and backward travelling waves returning from peripheral variances in the arterial system [88]. These forward and backward waves have been shown experimentally using both electrical and hydraulic models. In the electrical models, voltage has analogous behaviour to blood pressure and current has equivalent analogous to blood flow. Taylor experimentally showed that electrical and hydraulic models were mathematically equivalent when he compared an electrical transmission line to a single tube subject to sinusoidal fluid flow, the closed-end tube model [118, 117]. Jager et al. clarified the mathematics between the transmission line model and the arterial system by presenting similarities between the telegraph equations and the linearized Navier–Stokes

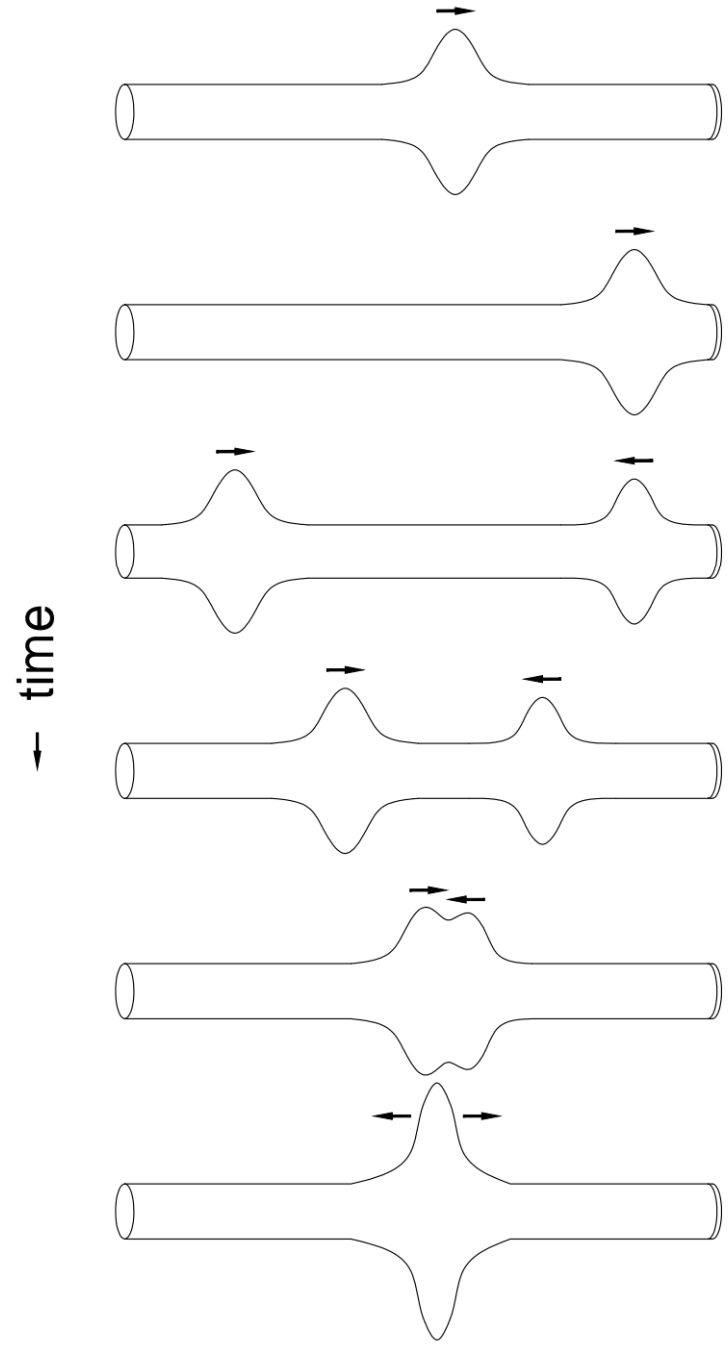

Figure 1.1: The closed-end tube model of the arterial system, adapted from McDonald's Blood Flow in Arteries: Theoretical, Experimental and Clinical Principles, Nichols, W.M. et. al., 6th edition, 2011, Hodder Arnold, London [88]. The heart ejects blood into the left side of a long elastic tube. For each heart beat, the pressure generated against the walls of the tube propagates down to the closed right side in a forward travelling pressure wave. Once the forward travelling pressure wave reaches the closed end of the tube, it is reflected backwards. The resulting backward travelling pressure wave sums with the forward travelling pressure wave generated by the subsequent heart beat.

equations [50]. The telegraph equations describe the transmission line and the linearized Navier–Stokes equations describe fluid flow. The telegraph and linearized Navier–Stokes equations are given in Appendix A and are shown to be analogous. The calculations for separating pressure and flow waves into their forward and backward travelling components were first outlined for a canine ascending aorta but now have been applied to humans, swine, and rabbits [57, 71, 88, 133]. The calculations from the canine study have been adapted to rat arteries in this thesis [133].

1.3.1 Wave Reflection Increases with Arterial Stiffness

Properties of the arterial system, including arterial stiffness, determine the amplitude and the velocity of propagation of the backward wave [88]. The amplitude of the backward wave is increased for stiff arteries. The velocity of propagation of the backward wave is increased for stiff arteries causing it to arrive during late systole, rather than diastole [88]. An example of age-related change in backward wave velocity between a father and his son is shown in Figure 1.2. The 68 year-old father has augmentation of aortic systolic blood pressure (SBP) from early backward wave arrival and the 37 year-old son has arrival of the backward wave during diastole [92]. The 68 year-old father has stiffer arteries than his 37 year-old son because of age-related degradation of the elastic components of his arteries. Stiffer arteries lead to negative cardiovascular outcomes including cardiac hypertrophy, rising blood pressure, and damage to vasodilated organs. This thesis examines methods of measuring arterial stiffness for basic science research on these cardiovascular outcomes.

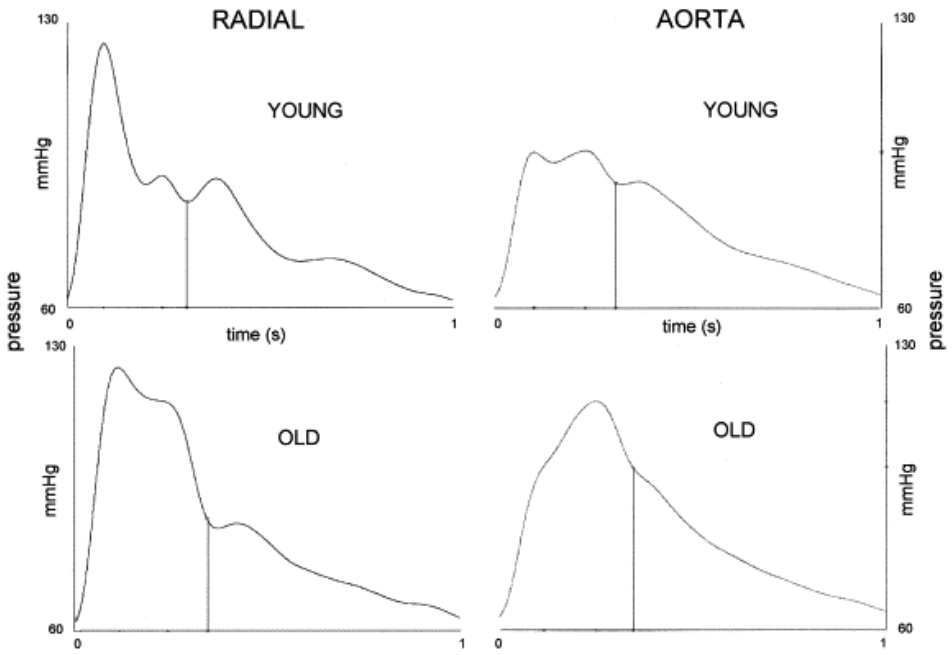

Figure 1.2: Radial (left) and aortic (right) pressure waves in a 36-year-old man (top) and his 68-year-old father (bottom) calibrated to the same brachial cuff values of systolic and diastolic blood pressure. Reprinted from the Journal of the American College of Cardiology, Volume 50, O'Rourke, M. F., and Hashimoto, J., Mechanical Factors in Arterial Aging: A Clinical Perspective, 1-13, Copyright (2007), with permission from Elsevier.

1.4 Measurement of Arterial Stiffness

Presently, there are several accepted approaches to measuring arterial stiffness: pulse wave velocity (PWV), pulse waveform analysis (PWA), wave separation analysis (WSA) and carotid ultrasonography [88, 127]. Pulse wave velocity uses the transmission speed of the pulse waveform as a direct measure of arterial stiffness. Pulse waveform analysis analyzes the shape of the measured pulse waveform, P_m, to indicate arterial stiffness. Wave separation analysis calculates wave reflection in the arterial system to indicate arterial stiffness. Wave separation analysis involves calculating P_f and P_b; it is also commonly referred to as impedance analysis. Pulse waveform analysis is the study of the shape of a pressure pulse, particularly the upward slope of each pulse, and does not involve separating the pressure pulse into forward and backward components. Carotid ultrasonography assesses structural changes in the arterial wall at the common carotid artery and its bifurcation [127]. The following sections discuss the principles, advantages, and disadvantages of these approaches in detail.

1.4.1 Pulse Wave Velocity

Pulsatile force increases with pulse wave velocity, which is the speed of the pressure wave travelling forward along an artery [88]. As the elastic modulus of the arterial wall increases, so does the pulse wave velocity by the Moens–Korteweg equation [88]:

$$PWV = \sqrt{\frac{Eh}{2R\rho}} \tag{1.2}$$

where E is the elastic modulus of the artery defined in Equation 1.1, h is the thickness of the arterial wall, R is the arterial radius, and ρ is the density of blood. In practice, pulse wave velocity is experimentally measured to obtain elastic modulus from Equation 1.2 [69]. Pulse wave velocity is measured by two methods: foot-to-foot transmission speed and local arterial imaging [69, 127].

The foot of a wave is usually defined as the end of diastole, where the upstroke from systole begins [69, 88]. The foot-to-foot transmission speed involves measuring a pulse wave at two separate locations, most commonly the right carotid and right femoral artery and calculating the time delay between the feet of the two waves [69, 127]. In other studies, different reference

points have been used to determine the time delay between waves [39, 97, 98], but these methods have been contested due to effects of wave reflection on the wave shape [40, 88, 134]. Pulse wave velocity is calculated by:

$$PWV = \frac{D}{\Delta t},$$

where D is the distance of the two arteries measured externally in meters and Δt is the time delay measured between the feet of the two waves [69]. The most common technique for measuring pulse wave velocity is the carotid-femoral foot-to-foot method [127].

An alternative approach to measure pulse wave velocity involves arterial imaging. Local arterial imaging using Doppler ultrasound or magnetic resonance imaging can be used to directly measure the local pulse wave velocity at an artery [37, 69, 75, 77]. One method of locally measuring pulse wave velocity is through measuring transit-time (TT). Transit-time is the time it takes for the pulse to travel from the heart to the area of arterial imaging. The pulse departing the heart is denoted by the ECG-R wave indicating ventricular contraction and the pulsed wave doppler upstroke indicates the arrival of the pulse at the area of arterial imaging. Transit-time does not have the same requirement of measuring the distance travelled by the pulse. Transit-time also has the added advantage that it only requires imaging one arterial site at a time and a simultaneous ECG trace. However, transit-time is only comparable between subjects when measured at the same arterial site in similar sized subjects. Transit-time is used in this thesis because it can be measured non-invasively and instantaneously in a time-sensitive drug injection experiment.

Pulse wave velocity measured at the carotid artery is desirable because the carotid artery is a common site of atherosclerotic plaque formation [12, 69]. However, local pulse wave velocity measured at the aorta is more accurate for patients with diabetes or hypertension [94]. Additionally, the magnitude of pulse wave velocity can be decreased in the carotid artery compared to the aorta due to decreased blood flow to the brain [64]. Both carotid and aortic pulse wave velocity have been shown to increase with concurrent cardiovascular disease and to predict risk of cardiovascular mortality in humans [32, 64, 68, 121, 123, 126]. However, the knowledge of whether these measures have the same predictive power in experimental animal models is unclear. Thus, the goal of this thesis is to examine and validate the use of

these measures in rodent models.

Pulse wave velocity is the gold standard for measuring arterial elasticity and, subsequently, arterial stiffness [69, 81, 125, 127]. The advantage to using pulse wave velocity is that it can be measured directly by ultrasound, whereas pulse waveform analysis and wave separation analysis derive arterial stiffness parameters through a model of the arterial system. The disadvantage to using pulse wave velocity to indicate arterial stiffness is that it varies with heart rate and blood pressure in multiple species [14, 66, 107, 115, 136].

1.4.2 Pulse Waveform Analysis

Pulse waveform analysis can be used as an indicator of arterial stiffness. Traditional and novel indicators of stiffness derived from pulse waveform analysis are explored in Chapter 2. Pulse waveform analysis uses the shape of the pressure waveform to infer arterial stiffness and, subsequently, the risk of cardiovascular disease and cardiovascular mortality. Currently used pulse waveform analysis parameters include diastolic blood pressure (DBP), systolic blood pressure, pulse pressure (PP), dP/dt_{max}, and augmentation index (AI_X). In the following section, Figure 1.3 illustrates the parameters of diastolic blood pressure, systolic blood pressure, pulse pressure, and dP/dt_{max}, and Equation 1.3 explains how to calculate AI_X. The shape of the measured pressure wave varies by anatomic location as illustrated in the representative arterial locations in Figure 1.2. Therefore, parameters of arterial stiffness measured from the shape of the pressure wave vary by anatomic location as well. For example, systolic blood pressure and pulse pressure measured invasively at central arteries have been shown to be better indicators of arterial stiffness than measured non-invasively at peripheral arteries [88]. Arterial stiffness has been associated with changes in pulse waveform analysis parameters: diastolic blood pressure, systolic blood pressure, pulse pressure, dP/dt_{max}, and AI_X.

Diastolic blood pressure, the nadir of the pressure pulse, is also dependent on arterial stiffness, peripheral resistance, and cardiac output [87]. An increase in arterial stiffness decreases diastolic blood pressure; a stiff arterial wall stores less potential energy during blood ejection from the heart [87]. The diastolic blood pressure decreases due to less potential energy from the arterial wall converting to kinetic energy during diastole [87]. In contrast, an increase in either peripheral resistance or cardiac output causes an increase in diastolic blood

pressure [87]. A decrease in diastolic blood pressure is seen in older patients with age-related arterial stiffness where wave-reflections have caused the backward wave to arrive during systole rather than diastole [30, 73, 76, 124]. An increase in diastolic blood pressure is used to indicate cardiovascular morbidity and mortality in young subjects where the strain on the heart is from increasing peripheral resistance rather than age-related arterial stiffening [73, 76, 124].

Systolic blood pressure, the peak of the pressure pulse, is dependent on arterial stiffness, peripheral resistance, and cardiac output [87, 88]. An increase in arterial stiffness increases systolic blood pressure by two different mechanisms: decreased force dampening from the central arteries and increased wave reflection. Systolic blood pressure rises when the central arteries are less able to convert the kinetic energy from blood ejection into potential energy [87]. Additionally, increased arterial stiffness increases the magnitude and transmission velocity of the backward pressure wave that causes an increase in systolic blood pressure because the backward pressure wave arrives during systole [87]. Similar to diastolic blood pressure, systolic blood pressure also increases with cardiac output and peripheral resistance [87, 88]. Systolic blood pressure is used as an indicator of the need for therapeutic intervention and to indicate cardiovascular morbidity and mortality [104, 112, 113, 137].

Pulse pressure is the difference between systolic blood pressure and diastolic blood pressure. Pulse pressure also increases with increasing arterial stiffness and can be used as an indicator of stiffness [88]. There are conflicting studies on whether pulse pressure is superior to systolic blood pressure in predicting cardiovascular morbidity or mortality [9, 61, 84]. Central arterial pulse pressure is a better indicator of arterial stiffness and predictor of cardiovascular morbidity and mortality in older adults [88].

The maximum time derivative of the pressure pulse waveform, dP/dt_{max}, has been used as a measure of arterial stiffness in peripheral arteries [4, 33, 34, 35]. In central arteries, dP/dt_{max} is used as a measure of left ventricular contractility [13].

The arteries stretch to accommodate the blood pushed by each contraction of the heart in systole. In diastole, the arteries recoil back to their original size. The portion of the pressure pulse waveform in diastole, the downward slope, occurs between peak systolic blood pressure and base diastolic blood pressure. The shape of the downward slope of the pressure pulse

waveform is influenced by the elastic recoil of the artery and presence of backward waves. The downward slope of the pressure pulse waveform is neglected in pulse waveform analysis because of the variation in shape imposed by the presence of backward waves; however, the steepest section of downward slope, dP/dt_{min}, could represent the maximum elastic recoil ability of the artery. In Chapter 2, the minimum time derivative of the pressure pulse waveform, dP/dt_{min}, is proposed as a novel measure of arterial stiffness in peripheral arteries. dP/dt_{min} could be a better indicator of arterial stiffness than dP/dt_{max} because the elastic recoil of the artery occurs in a passive portion of the cardiac cycle, diastole, where the active contraction of the heart does not have a direct effect.

$\mathrm{AI_X}$, a measure of wave reflection, increases with arterial stiffness and predicts cardiovascular morbidity independent of peripheral pulse pressure [125]. $\mathrm{AI_X}$ measures the boost in late systolic blood pressure from the backward wave arrival expressed as a percentage:

$$\mathrm{AI_X} = \frac{\mathrm{AP}}{\mathrm{SBP} - \mathrm{DBP}} \times 100, \tag{1.3}$$

where AP is the amplification pressure. AP represents the increase in pressure measured by the difference in amplitude of the systolic blood pressure and forward pressure wave (A_f) shown in Figure 1.3. The forward pressure wave height is estimated by an inflection point that indicates the arrival of the backward wave. The inflection point is defined as the second peak of the second derivative of the pressure wave, is denoted as P_{infl} in the literature, and is shown in Figure 1.3 [88]. AP is calculated by:

$$\mathrm{AP} = \mathrm{SBP} - P_{infl}.$$

In human medicine, $\mathrm{AI_X}$ is used to estimate of the size of the backward wave based on a well-known blood pressure wave shape [88]. Generally, $\mathrm{AI_X}$ is measured in the aorta but several studies have measured $\mathrm{AI_X}$ in peripheral arteries with conflicting results [72, 114]. Aortic $\mathrm{AI_X}$ is influenced by many factors: heart rate, aortic taper, body length, and left ventricular ejection [38, 88]. In this thesis, the blood pressure data were collected from the carotid and femoral arteries in rats did not meet the shape requirements to measure $\mathrm{AI_X}$. Therefore, other pulse waveform analysis parameters are vital tools for basic science research in arterial stiffness. Chapter 2 explores pulse waveform analysis parameters in rats, including a new

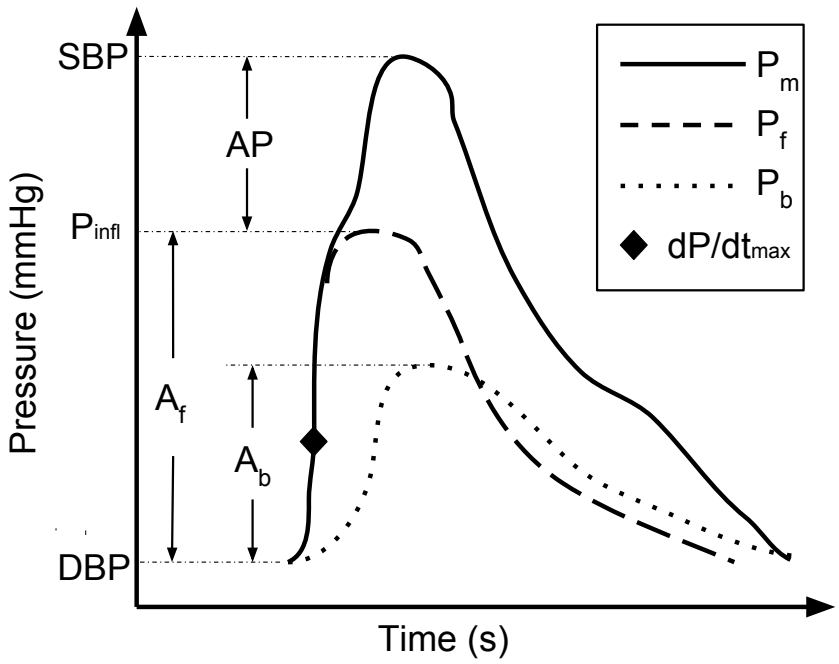

Figure 1.3: Schematic blood pressure waveform showing measured (P_m), forward (P_f) and backward (P_b) arterial pressure waves, systolic blood pressure (SBP), diastolic blood pressure (DBP), amplification of the pressure pulse (AP), amplitude of the forward pressure wave (A_f), amplitude of the backward pressure wave (A_b), and maximum time derivative of pressure (dP/dt_{max}, i.e., the slope of the increase in pressure with each pulse). The arrival of the backward wave is estimated by a change in systolic upstroke pressure called the inflection point (P_{infl}). Reflection index (RI = $A_b/(A_f+A_b)$) and augmentation index ($\text{AI}_\text{X}= AP/(SBP - DBP) \times 100$) can be calculated from AP, A_f, and A_b.

proposed pulse waveform analysis parameter, the minimum time derivative of the pressure pulse waveform, dP/dt_{min}.

1.4.3 Wave Separation Analysis

Wave Separation Analysis can be used to derive indices of arterial stiffness. The use of wave separation analysis is novel in rats and thus will be explored in Chapter 4. Wave separation analysis involves the calculation of forward and backward pressure waves from a measured pressure wave [127]. The forward and backward pressure waves can be calculated from a measured pressure wave if there are simultaneous flow waves also measured or estimated in the same animal [132]. Flow is needed along with pressure in wave separation analysis

in order to calculate characteristic impedance (Z_c), which is a measure of the resistance at an artery immediately distal to the measuring site to pulsatile blood flow. Characteristic impedance is defined as the ratio of oscillatory pressure to oscillatory flow assuming no wave reflections are present [133]. Determining the characteristic impedance at an artery is the first step in the calculation of forward and backward waves. Once the forward and backward waves are calculated, their ratio, the reflection index (RI), can be used as a measure of arterial stiffness. Chapter 3 describes the mathematics of wave separation analysis in detail.

Wave separation analysis parameters include Z_c, RI, and backward pressure wave amplitude. Wave separation analysis parameters are not interchangeable with pulse waveform analysis parameters. For example, RI has a better predictive ability for adverse cardiovascular morbidity and mortality than AI_X [127]. Wave separation analysis parameters that quantify the degree of wave reflection, backward pressure wave amplitude, and RI are recommended vascular biomarkers for predicting cardiovascular morbidity and mortality [127, 129].

Z_c is used to determine the stiffness of an artery immediately distal to the measuring site [88]. Z_c increases as an artery becomes stiff. If an artery diameter increases, Z_c decreases [88]. The characteristic impedance of the aorta is also used as a measure of left ventricular after-load, that is, the pressure the left ventricle must contract against to eject blood [88]. The characteristic impedance of peripheral arteries is a measure of the difficulty for the blood to pass through that artery [88]. In rodents, Z_c has been measured in the aorta to study cardiovascular disease [67, 80, 105]. This thesis proposes a new approach in Chapter 4 that allows Z_c measurement in the carotid and femoral arteries of a rat. There are multiple methods to calculate Z_c. These methods and the details of the specific method used to calculate Z_c are complex. Due to the complexity of the Z_c derivation, Z_c is not as favoured as a measure of arterial stiffness compared to pulse waveform analysis. Chapter 3 in this thesis is devoted entirely to detailing the method used in this thesis for Z_c calculation. Chapter 3 will not be a publication, but it is necessary to understand in detail the contents of Chapter 4, a manuscript examining wave separation analysis use in a rat model.

RI represents the ratio of the backward wave to the measured wave and is calculated by:

$$RI = \frac{A_b}{A_f + A_b},$$

where A_b is the amplitude of the backward pressure wave and A_f is the amplitude of the forward pressure wave. Reflection index has been shown to be predictive of cardiovascular mortality in men but not in women [129].

Reflected pressure amplitude measures the magnitude of the wave reflections. Reflected pressure amplitude has been shown to be an indicator of arterial stiffness, cardiovascular morbidity, and mortality, independent of gender [127, 129].

The manuscript in Chapter 4 outlines wave separation analysis in the rat. A method in rats for calculating Z_c has been outlined [80] and is currently in use [24, 105].

1.4.4 Carotid Ultrasonography

Carotid ultrasonography involves directly imaging the common carotid artery using transcutaneous ultrasound in greyscale (B-mode) and Doppler modes [36]. The two main carotid ultrasonography parameters are the carotid intima-media thickness (cIMT) and carotid peak systolic velocity (CA PSV) [99].

cIMT is the distance between the intimal and adventitial arterial wall layers measured transcutaneously with grey scale ultrasonography [127]. cIMT measures the local atherosclerosis of the carotid artery and is used a surrogate measure of generalized atherosclerosis [127].

CA PSV is a measure of the peak velocity of blood through the carotid artery [36]. CA PSV is a measure of the narrowing of the carotid artery, carotid artery stenosis, that occurs with carotid plaque formation and increased cIMT [99].

Carotid ultrasonography is widely used to evaluate arterial stiffness and cardiovascular morbidity because it is non-invasive and relatively inexpensive [36, 99, 127]. However, there are many inconsistencies in ultrasound examination protocol [36]. Within the same laboratory, extreme care must be taken to follow a consistent protocol for all carotid ultrasound examinations. In this thesis, CA PSV was measured to give a general measure of the degree of carotid artery stenosis throughout the carotid artery.

1.5 Rats as a Model Species for Cardiovascular Toxicology and Pharmacology Studies

The ideal animal model for translational cardiovascular research mimics human pathophysiology and develops the same end-stage disease as humans [103]. Economically, it is desirable for an animal model to be small with a short lifespan; however, the animal model must be large enough to perform the desired measurements to be practical [103].

Rodents and lagomorphs are important models for cardiovascular disease. Arterial stiffness has been assessed in rats for many pathophysiological states, including aging, left ventricular hypertrophy, hypertension, calcification of arteries, chronic renal failure, and diabetes [18, 19, 24, 44, 67, 90, 105]. Normal rats, mice, and rabbits are resistant to atherosclerosis [103]. A variety of genetic strains of rats (i.e., Zucker Diabetic Fatty, spontaneously hypertensive rats, and cp/cp), mice (i.e., APoE-/- and LDLR-/-) and rabbits (i.e., watanabe heritable hyperlipidemic and Kurosawa and Kusanagi-Hypercholesterolemic) have been developed to model the abnormal metabolism associated with atherosclerotic disease in humans [54, 103].

Atherosclerosis can also be induced in common strains of rodents and lagomorphs. Rabbits are sensitive to a high cholesterol diet and will develop atherosclerotic lesions in response to increased cholesterol in the diet [103]. Atherosclerosis has also been induced in normal rats and mice for toxicology and pharmacology studies with high cholesterol diets, and excess vitamin D in combination with nicotine [22, 45, 51, 103]. Vitamin D given as a single agent has a variety of effects on the vascular system. Vitamin D has a protective effect on the arterial system by suppressing inflammatory processes [140]. Deficiency of vitamin D leads to an inflammatory state where the arterial system is predisposed to atherosclerotic plaques of activated endothelial cells and vascular smooth muscle cells [140]. However, vitamin D given in excess causes calcification of the arteries [140]. In this thesis, rodents with a variety of levels of vitamin D supplementation were used to study methods of measuring arterial stiffness because of the range in arterial stiffness created.

1.5.1 Arterial Stiffness Measurement in Rats

Pulse wave velocity has been used to measure arterial stiffness in the rat, using both invasive and non-invasive methods [14, 81]. Measuring pulse wave velocity with two catheter-tip manometers placed in the aorta and the foot-to-foot time delay method has highly reproducible results in rats [81]. This invasive technique has been used to verify that pulse wave velocity is heart rate and pressure dependent in rats [14, 115]. Non-invasive techniques for measurement of pulse wave velocity in rats involve using doppler ultrasound and simultaneously recorded ECG to calculate transit speed of the pulse over a known distance [83]. Chapter 2 uses non-invasive pulse wave velocity to measure arterial stiffness.

The pulse waveform analysis parameter AI_X has been used to study arterial stiffness in a rat model of type 2 diabetes; however, AI_X was calculated with the software SphygmoCor 8.0 (AtCor Medical, Sydney, Australia) that is developed and verified for the human radial artery [6, 78]. AI_X has also been calculated in rats by inspection of the return point of the backward wave in central aorta pressure recordings [89]. In this thesis, AI_X was not measured because the blood pressure data collected from the carotid and femoral arteries in rats did not have the required pulse waveform shape. The pulse waveform analysis parameter, dP/dt_{max}, has been used as a measure of arterial stiffness in toxicology studies in rats [33, 34, 35]. A novel pulse waveform analysis parameter dP/dt_{min} is investigated in rats in Chapter 2.

Wave separation analysis has been used to verify that a new advanced glycation inhibitor, LR-90, prevented arterial stiffening and to investigate the effect of nitric oxide on the arterial system [16, 43, 105]. The use of wave separation analysis parameters, characteristic impedance, reflection index, and wave transit time were verified by histological examination of the rat aorta in two independent studies [24, 105]. Accumulation of advanced glycation end products were observed in rats that also had increased reflection index and wave transit time [24, 105]. These advanced glycation end products bind and induce alterations on proteins and lipid structures of the arterial wall [24, 105]. Once advanced glycation end products are bound to the arterial structures they interact with their receptor (RAGE) that cause arterial stiffening through reactive oxygen species generation and activation of the immune response [24, 105]. Additionally, left ventricular hypertrophy has been shown to occur in

rats with artificially increased wave reflection through surgical aorta narrowing [60]. A novel technique for performing wave separation analysis in rats is presented in Chapters 3 and 4. The technique will allow measurement of characteristic impedance, backward wave amplitude, and reflection index in the peripheral arteries for improved understanding of arterial stiffness in dynamic cardiovascular studies in the rat.

Carotid ultrasonography has been used in rats to investigate the risk of early salt exposure on hypertension and stroke risk and the effects of arterial injury on arteriosclerosis [28, 62]. Spontaneously hypertensive rats fed a high-fat diet have been used to verify cIMT measurements captured by high-frequency ultrasound against carotid artery intima thickness measured by histology [23]. CA PSV has been used as a measure of blood flow and an indicator of shear stress through the carotid artery in rats after arterial injury [62]. More commonly, CA PSV is used to indicate carotid artery stenosis [36]. In Chapters 2 and 4, CA PSV is used to measure arterial stiffening, which causes a stenotic-like condition.

1.5.2 Blood Pressure Measurement in Rats

Blood pressure in rats can be measured by a variety of techniques: tail cuff oscillimetry, implantable telemetry, and intra-arterial catheterization. Of these three techniques, intra-arterial catheterization is the gold standard of blood pressure measurement [95].

Tail cuff oscillimetry is the indirect measurement of blood pressure at the tail artery by an oscillemetric cuff [42]. Tail cuff oscillimetry blood pressure is highly variable with rat body temperature [42]. During tail cuff oscillimetry, the rectal temperature of the rat must be kept between 34 °C and 36 °C for five minutes to obtain an accurate measurement of blood pressure [42]. If direct blood pressure is measured, the rats can be normothermic during blood pressure measurement [42]. Variability between tail cuff oscillimetry and direct blood pressure measurement of systolic blood pressure has been reported to be as high as 34 mmHg [63]. Tail cuff oscillimetry is recommended for detecting substaintial group differences in systolic blood pressure and systolic blood pressure changes in large numbers of animals [65]. Tail cuff oscillimetry is not recommended for measuring diastolic blood pressure or pulse pressure and therefore was not used in this thesis [65].

Implantable telemetry directly measures blood pressure by an implantable radio trans-

mitter [46]. Implantable telemetry is desirable for chronic, continuous blood pressure measurement and has an added advantage that rats do not have to be restrained or anaesthetized during data collection [46]. The blood pressure data from implantable telemetry are accurate enough to study subtle changes in blood pressure [65]. A disadvantage of implantable telemetry is that it involves a surgical procedure with a prolonged surgical recovery time, possibility of significant complications, and the possibility that catheters can lose their patency over long studies [48]. The largest roadblock for researchers that want to use implantable telemetry is the expense and labour associated with using this technique compared to other methods (tail cuff oscillimetry, intra-arterial catheterization) [65]. In this thesis, implantable telemetry is used to investigate pulse waveform analysis parameters dP/dt_{min} and dP/dt_{max} in conscious, unrestrained rats.

Intra-arterial catheterization is the direct measurement of arterial blood pressure using a heparinized saline-filled catheter attached to a pressure transducer or Millar solid-state high-fidelity catheter [95]. The disadvantage to intra-arterial catheterization is that it involves a surgical procedure that is usually performed under anesthesia and is often terminal [48]. Millar catheters are preferred over heparinized saline-filled catheters because heparinized ssaline-filled catheters are subject to errors from variable damping due to air micro-bubbles in the catheter [88]. Millar catheters were used in this thesis to study wave separation analysis because they will not introduce artificial errors into the wave separation analysis algorithm due to dampening.

1.6 Study Rationale

This thesis conducts two studies intended to increase the information available in the field of cardiovascular preclinical biomedical science pertaining to arterial stiffness. The first study in Chapter 2 presents a novel measure of arterial stiffness, dP/dt_{min}. The validity of dP/dt_{min} as a measure of arterial stiffness is investigated with chronic changes in arterial stiffness through a rodent model of vitamin D deficiency and vitamin D excess. Radio-telemetry is used to obtain accurate 24-hour blood pressure measurements in conscious unrestrained rats for the study. The responsiveness of dP/dt_{min} for acute changes in arterial stiffness is also

assessed by vasoactive drug injection in anesthetized rats. The goal of the first study is to provide a sensitive measure of arterial stiffness in rats where intra-arterial blood pressure is measured. The second study presents a novel technique for measuring wave separation analysis parameters that indicate arterial stiffness. The aim of the novel technique is to measure wave separation analysis parameters in easily accessible arteries such as the femoral artery. The wave separation analysis algorithm is outlined, developed, and tested against a known dataset in Chapter 3. The surgical portion of the novel wave separation analysis technique is validated in normal male Wistar rats in an acute vasoactive drug injection experiment in Chapter 4. The goal of the second study is to add wave separation analysis to the arsenal of tools available to preclinical biomedical researchers to ensure human clinical end-points reflect those obtained in preclinical biomedical research. Human clinical end-points are based on non-invasive pulse wave analysis techniques developed to estimate arterial stiffness in the central arteries that have not been validated in a rodent models [6]

1.7 Research Hypotheses

This thesis investigates the following hypotheses:

1. Chronic changes in the vascular wall can be measured by dP/dt_{min}. A increase in arterial stiffness will cause an increase in magnitude of dP/dt_{min}.

2. Acute changes in the vascular wall can be measured by dP/dt_{min}. A increase in arterial stiffness will cause an increase in magnitude of dP/dt_{min}.

3. Backward waves can be measured in the femoral artery in rats.

4. The backward wave amplitude measured in the femoral artery in rats increases with an increase in arterial stiffness.

1.8 Research Objectives

The objectives are as follows:

1. Outline the theory behind wave separation analysis in a precise, rigorous manner.
2. Develop a peripheral artery technique for wave separation analysis in the rat.
3. Develop open source software to calculate dP/dt_{min} and the wave separation analysis parameters.
4. Perform acute experiments to validate whether that dP/dt_{min} and backward wave amplitude are superior measures of arterial stiffness or not.

Chapter 2

Arterial Pressure dP/dt_{min} as a Novel Measure of Arterial Stiffness in a Rodent Model of Vitamin D Excess

The following study will be submitted to the Journal of Pharmacological and Toxicological Methods. Replication of some material from the introduction is unavoidable. This manuscript describes a new measure of arterial stiffness, dP/dt_{min}, in the rat that is based on analyzing the shape of the pressure wave; i.e., pulse waveform analysis. I contributed 90% of the manuscript. I developed the software, analyzed the data, prepared figures, and drafted the manuscript. Lynn P. Weber and I designed the research study, interpreted results of experiments, and edited and revised the final version of this manuscript. Nagmeh Z. Mirrhosseini and I performed the experiments and collated the data. This chapter also contains a description of the software development process and verification in Section 2.2.6.

2.1 Introduction

Epidemiological studies have shown that arterial stiffness is associated with increased morbidity and mortality in humans [53, 96]. Diseases caused by arterial stiffness include cardiac failure [67], hypertension [53], small vessel disease of the kidney leading to renal failure, and small vessel disease of the brain leading to dementia [82, 96]. Inflammation and aging causes the artery to become stiff due to structural thickening and calcification [79, 92, 139]. Age-related elastic structural protein damage transfers stress from elastin to collagen fibers that have a higher elastic modulus contributing to stiffening of the arterial wall [7, 55]. Vitamin D

excess has been shown to calcify rodent arteries [51, 58, 140], resulting in arterial stiffening. Vitamin D deficiency has also been shown to stiffen arteries in humans [1]. Vitamin D deficiency and excess versus normal vitamin D was used to provide a range of arterial stiffness in rats in this study.

Blood pressure telemetry provides sensitive pulse waveform data from rodents in research trials, which may be used to predict changes in arterial stiffness in humans. The shape of the arterial pulse waveform changes with the elasticity of the artery because the effectiveness of the vessel wall to dampen the pulsatile force of blood is altered (Fig. 2.1; adapted from [92]). The maximum time derivative of blood pressure (dP/dt_{max}), i.e., the maximum rate of increase of pressure of the pulse waveform has been extensively used as a measure of arterial stiffness in this laboratory and others [4, 33, 34, 35]. In other studies, the minimum time derivative of blood pressure (dP/dt_{min}), i.e., the maximum rate of decrease of pressure of the pulse waveform has been used to indicate rate of left ventricular relaxation [74, 138]. dP/dt_{min} indicates left ventricular relaxation when measured in the aorta immediately distal to the left ventricle [74, 138]. This study measures dP/dt_{min} farther from the heart (i.e., in the iliac artery). In the iliac artery, dP/dt_{min} no longer measures ventricular relaxation, and we hypothesize that it will be indicative of arterial stiffness.

The objective of this study is to determine whether dP/dt_{min} can detect acute changes in the vascular wall as well as or better than dP/dt_{max}. To compare dP/dt_{min} and dP/dt_{max}, rodent models of vitamin D excess and deficiency were used to create a range of arterial stiffness. Arterial pressure was measured using a blood pressure telemetry catheter inserted into the iliac artery in rats fed varying levels of vitamin D for four weeks. The effectiveness of pulse waveform dP/dt_{min} versus dP/dt_{max} as indicators of arterial stiffness was evaluated by correlating with carotid peak systolic velocity, CA PSV, of the same rats at baseline and week four. CA PSV is a measure of stenosis of the carotid arteries and vitamin D excess or deficiency causes arterial stiffening, a stenotic-like condition [1, 51, 36]. Therefore, CA PSV can be used as an indicator of arterial stiffening in this study to compare dP/dt_{min} and dP/dt_{max} values for validation. The ability of dP/dt_{min} to detect changes in the vascular wall was then verified by measuring dP/dt_{min} and dP/dt_{max} following administration of vasoactive drugs acetylcholine (Ach) and norepinephrine (NE).

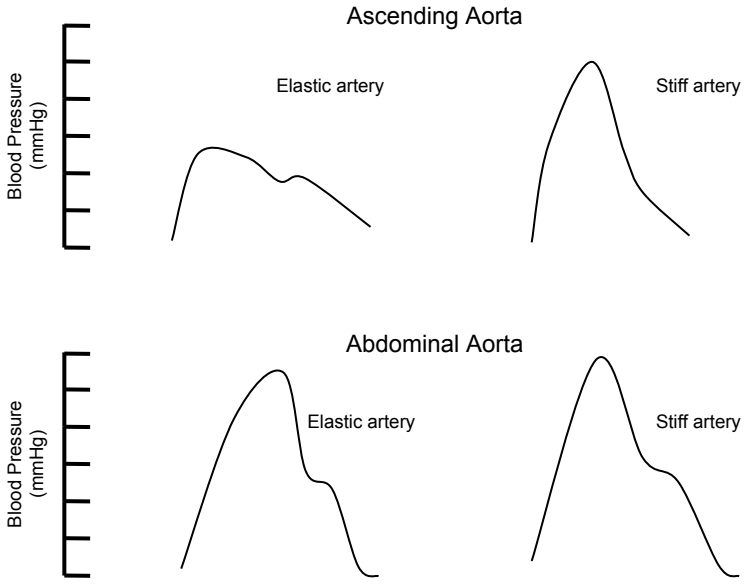

Figure 2.1: Theoretical pulse waveform in stiff (right side) versus elastic (left side) arteries. The shape of the pulse waveform changes depending not only with differing degrees of stiffness, but also on location within the vascular tree. Compare a typical trace if the pressure catheter is placed in the ascending aorta (top traces) versus in the abdominal aorta (bottom traces).

2.2 Methods

2.2.1 Animal Surgery and Care

This work was approved by the University of Saskatchewan Animal Research Ethics Board and adhered to the Canadian Council on Animal Care guidelines for human use. Twenty male Wistar rats (150-450g) for Experiment 1 and four Male Sprague-Dawley rats (300-360g) for Experiment 2 were housed individually and provided food and water ad libitum. Rats were allowed to acclimatize five days before surgical implantation of blood pressure telemetry devices using the method of Gentner and Weber [33]. The Wistar rats were premedicated with Buprenorphine (20 μg/kg s.c.; Reckitt Benckiser Healthcare Ltd., Hull, UK); the Sprague-Dawley rats were premedicated with Buprenophrine (20 μg/kg i.m.; Schering-Plough, Hert-

fordshire, UK) and Midazolam (0.2 mg/mL i.m.; Sandoz Canada, Inc., Boucherville, Que.). Surgical anesthesia was induced with 5% isoflurane and 1 L/min of oxygen and maintained at 0.5-2% isoflurane and 0.5 L/min of oxygen. Trivetrin (30 mg/kg s.c.; Schering Canada Inc., Pointe-Claire, Qubec) was administered prior to starting surgery. A PA-C10 transmitter (Data Sciences International, St. Paul, Minn.) was implanted in the femoral artery and advanced to the iliac artery caudal to the iliac bifurcation, with the transmitter body placed subcutaneously in the left flank. Post-operative support included replacement fluids (5-15 mL saline s.c. in a 24 hour period for two days following surgery), buprenorphine (20 μg/kg s.c. every 12 hours up to 48 hours), thermal support for 1 hour, and Trivetrin (30 mg/kg s.c. daily for six days). Rats were allowed to recover for seven days post-surgery before entering the study.

2.2.2 Experiment 1: Chronic Vitamin D Experiment

After surgical recovery, blood pressure and cardiac ultrasound measurements were performed in the untreated Wistar rats (150-450g) to record a baseline measurement and performed after four weeks of feeding diets with varying levels of vitamin D. Rats were split into five groups of n=4 where each group received a different vitamin D diet. The Vitamin D diets had exact dosages of 1,25-dihydroxyvitamin D (0 IU/g, 0.4 IU/g, 6.7 IU/g, 20 IU/g, and 100 IU/g) in a nutritionally complete rat diet (Harlan Laboratories, Madison, WI). The dietary levels of vitamin D were chosen to provide each rat with a vitamin D dose equivalent to the human doses that correspond to deficiency, the recommended daily intake, the maximum therapeutic dose, the lower toxic limit and the upper toxic limit, respectively. The 0.4 IU/g recommended daily intake vitamin D diet served as the control group. The vitamin D diets fed to the rats did not cause any physical signs of illness or distress (poor grooming, lack of appetite, decreased appetite, and stereotypic behaviour) during the study. At the end of the experiment, the rat body weights and food consumption did not differ among groups.

2.2.3 Experiment 2: Vasoactive Drug Experiment

After recovery from surgical implantation of blood pressure telemetry devices, four Male Sprague-Dawley rats (300-360g) were used in an acute drug injection experiment. Anesthesia was induced with 5% isoflurane then maintained at 3% isoflurane to examine the effects on dP/dt_{min} and dP/dt_{max} of bolus injections of vasoactive drugs: ACh and NE and a saline vehicle. Arterial blood pressure was recorded while a saline vehicle (0.5 mL/kg), ACh (0.91 ng/kg), and then NE (0.02 mg/kg) were intravenously injected into the tail vein [33]. A five-minute washout period after blood pressure had returned to pre-injection values was used between injections.

2.2.4 Pulsed Wave Doppler Procedure

Pulsed wave Doppler ultrasound at the carotid artery was performed to obtain CA PSV using a Vevo 660 high-frequency ultrasound (VisualSonics, Markham, ON) equipped with B-mode and Doppler imaging. Each ultrasound procedure took less than 30 minutes for each animal. Prior to the ultrasound experiments, rats were anesthetized with 5% isoflurane and were maintained at 0.5-3% isoflurane (Abbott Laboratories, Saint-Laurent, QC). Once anaesthetized, the animals were placed in dorsal recumbency on an electrocardiogram (ECG) plate (VisualSonics, Markham, ON) with each paw covered with electrode cream (Signa Crme, Parker Laboratories, Fairfield, NJ) and secured to ECG contacts with surgical tape to monitor heart rate throughout the entire experiment. A heated platform maintained an internal body temperature of 37 ^{o}C as measured by a rectal temperature probe throughout the ultrasound procedure. To reduce ultrasound image artifacts, hair was removed by wiping the chest area after five minutes of depilatory cream treatment (Nair, New York, NY). EcoGel 200 (Eco-Med Pharmaceuticals, ON) was then applied to the thorax for ultrasound. A RMV 710B scanhead was used to first locate the right carotid artery at the level of its bifurcation in B-mode and then a pulsed wave Doppler trace was obtained. The CA PSV was calculated from the average peak velocity of three representative peaks. The averaged CA PSV was then used per rat in a weekly time-point in subsequent statistical analyses.

2.2.5 Pulse Waveform Analysis

The blood pressure data were analyzed using in-house software written specifically for these experiments (`PWanalyze` software). The `PWanalyze` software uses 6th order central differences to calculate the derivatives for the measures dP/dt_{min} and dP/dt_{max}. This software has been released for free and is available at http://sourceforge.net/projects/PWanalyze under the GNU public license.

In the chronic vitamin D experiment, arterial blood pressure was recorded at baseline and at week four. The arterial blood pressure recordings were from continuously sampling blood pressure-telemetry data in conscious unrestrained rats for five minutes every hour for 24 hours. Each five minute reading every hour was analyzed to measure both dP/dt_{min} and dP/dt_{max}. The values of dP/dt_{min} and dP/dt_{max} over the entire 24 hour period were then used per rat in subsequent statistical analyses. Waveforms that were artifacts were excluded from the data analysis. A waveform was considered an artifact if there was gap in the sampling from the rat telemetry device during a pressure pulse. Those rats with pressure waveforms that consisted of more than 15% artifacts in the total trace were excluded from the study to prevent error from blood pressure telemetry transmitter failure. Rats from groups 0 IU/g and 20 IU/g were excluded due to transmitter failure. Eighteen rats were part of the final sample size for this experiment. The remaining rats included three in the 0 IU/g group, four in the 0.4 IU/g group, four in the 6.7 IU/g group, three in the 20 IU/g group, and four in the 100 IU/g group. In the acute drug injection experiment, 30 second segments before and after drug injections were analyzed. The pre-injection and post-injection values of dP/dt_{min} and dP/dt_{max} over the 30 seconds were then used in statistical analysis.

2.2.6 Software Development

`PWanalyze` software was developed in Python 2.7, a high-level interpreted language [122]. Python is designed for development productivity and is supported by a large community of software developers. `PWanalyze` used several widely distributed packages including `Numerical Python` for ease of mathematical operations, `matplotlib` for graphing, and `wxpython` for a graphical user interface [5, 47, 102]. `PWanalyze` software uses 6th order central differences

to calculate the derivatives for the measures dP/dt_{min} and dP/dt_{max}. To verify that the derivatives were correct, `PWanalyze` was tested with periodic functions with known analytical derivatives and varying domain discretizations.

The user of `PWanalyze` is able to specify a data file to be analyzed. A sample data file showing the desired CSV format is provided with the software release. The data are displayed graphically such that the user is able to navigate the blood pressure trace and select a portion of the trace to be analyzed. `PWanalyze` then calculates dP/dt_{min}, dP/dt_{max}, systolic blood pressure, diastolic blood pressure, pulse pressure, and heart rate. The results of the analysis are displayed directly on the blood pressure trace as shown in Figure 2.3 and in text format in an analysis log for further statistical analysis. Both the graphical blood pressure trace and analysis log can be saved at any time in the analysis process by the user. `PWanalyze` is a freely available tool for researchers using rats to investigate cardiovascular disease to calculate traditional measures of arterial stiffness, dP/dt_{max} and the novel measure dP/dt_{min}.

2.2.7 Statistical Analysis

All measurements are reported as a median and range. In the chronic vitamin D experiment, the effects of individual variation on the measurements were removed by using a percent change from baseline to week four for each of the parameters prior to statistical analysis. Spearmans correlation and Bland-Altman analysis were used to compare dP/dt_{min} and dP/dt_{max} to CA PSV [11]. All Spearmans correlations and Bland-Altman analyses were performed using 36 independent measures in total, i.e., baseline and final measurement in 18 different rats. Correlations with $r > 0.6$ were considered to show a strong relationship. The Bland-Altman analysis 95% limits of agreement was reported as a mean bias $\pm$ 2 standard deviations. Comparisons between groups to measure treatment effects were calculated using a Kruskal Wallis test followed by Mann-Whitney U-test corrected for multiple comparisons by Bonferonni's method. In the acute drug injection experiment, the effects of each drug were investigated by using the difference between pre-injection and post-injection parameter values prior to statistical analysis. The Kruskal Wallis test followed by Mann-Whitney U-tests corrected for multiple comparisons by Bonferonni's method were used to compare treatment effects. Statistics were performed using R [100]. Results with $p < 0.05$ were considered to

be statistically significant.

2.3 Results

The values at baseline for systolic blood pressure, diastolic blood pressure, pulse pressure, heart rate, and CA PSV in the chronic vitamin D experiment were 120 (105-305) mmHg, 91 (77-101) mmHg, 33 (14-39) mmHg, 363 (258-420) bpm and 646 (261-794) cm/s, respectively, for all groups combined (n=18 rats). The change from baseline to the end of the experiment for systolic blood pressure, diastolic blood pressure, pulse pressure, heart rate, and CA PSV values for each treatment group is shown in Table 2.1. The measured CA PSV range (321-909 cm/s) indicated that arterial stiffness at the end of the experiment was sufficiently varied to explore the comparability and potential superiority of dP/dt_{min} versus dP/dt_{max} as indicators of arterial stiffness. Before exploring this comparison, we first examined more traditional measures of arterial stiffness (CA PSV, systolic blood pressure, and pulse pressure). Systolic blood pressure varied significantly between groups. Systolic blood pressure showed a trend for increase in 0, 6.7 and 100 IU/g/day groups compared to control (normal diet) (Table 2.1). However, it should be noted that systolic blood pressure increases in response to many factors in addition to increased arterial stiffness, including increased cardiac output or increased diastolic pressure, so it is not a reliable indicator of arterial stiffness. Diastolic pressure varied significantly between groups with treatment. Diastolic blood pressure is not generally considered to be reflective of arterial stiffness; however, there was a trend for increase at the highest vitamin D dose group compared to control (Table 2.1). Pulse pressure was not significantly different from control in any treatment group, indicating that this measure of arterial stiffness was relatively insensitive. Heart rate is not an indicator of arterial stiffness, but does confound interpretation of increases in systolic blood pressure, pulse pressure, and CA PSV if it is significantly altered with treatment. Although there are trends for change, heart rate was highly variable and showed no significant differences among treatment groups (Table 2.1). Finally, the clinically important CA PSV showed a trend for increase in the 0, 6.7, and 100 IU/g/day groups compared to control, but was not significant (Table 2.1). The pulsed wave Doppler trace of a rat in the 0 IU/g treatment group showed greater CA PSV

Table 2.1: Traditional measures of arterial stiffness and blood pressure for each treatment group reported as change from baseline at the end of the experiment, where pulse pressure is denoted as PP, carotid peak systolic velocity is denoted as CA PSV, and heart rate is denoted as HR. Values reported as median and range in parentheses. The 0.4 IU/g Vitamin D diet is the control.

Treatment	ΔSystolic Blood Pressure (mmHg)	ΔDiastolic Blood Pressure (mmHg)	ΔPP (mmHg)	ΔCA PSV (cm/s)	ΔHR (bpm)
0 IU/g n=3	12 (6-14)	7 (3-9)	3 (-1-11)	89 (-148-281)	-36 (-59- -4)
0.4 IU/g control n=4	-1 (-5-4)	5 (2-17)	-7 (-14- -4)	-128 (-218-26)	6 (-41 - 42)
6.7 IU/g n=3	8 (8-9)	8 (5-10)	0 (3-4)	90 (-13-305)	16 (-11-50)
20 IU/g n=3	2 (2-6)	4 (3-5)	0 (-2-2)	-7 (-69-54)	-55 (-80- -54)
100 IU/g n=4	15 (8-25)	17 (12-21)	-3 (-12-15)	125 (52-405)	-26 (-53-53)

Note: The Kruskal-Wallis test was significant for a treatment differences in systolic blood pressure ($p = 0.009$) and diastolic blood pressure ($p = 0.041$).

Table 2.2: `PWanalyze` calculated measures of arterial stiffness, dP/dt_{max} and dP/dt_{min} for each treatment group at the end of experiment. Values reported as median and range in parentheses. The 0.4 IU/g Vitamin D diet is the control.

Treatment	dP/dt_{max} (mmHg/s)	dP/dt_{min} (mmHg/s)
0 IU/g n=3	1678 (555-2148)	-738 (-785- -290)
0.4 IU/g control n=4	1055 (808-2765)	-481 (-883- -413)
6.7 IU/g n=3	2256 (1281-2710)	-813 (-1020- -588)
20 IU/g n=3	2290 (2048-2534)	-858 (-888 - -815)
100 IU/g n=4	1651 (1045-1944)	-704 (-812- -501)

measured after four weeks compared to CA PSV measured before entry into the study; see Figure 2.2. The increase in CA PSV indicates that arterial stiffening has occurred during the trial because of the 0 IU/g vitamin D diet. Taken together, although these traditional indicators of arterial stiffness showed the expected direction of change, the sensitivity for detecting significant increases was not great, requiring highly toxic levels of vitamin D for consistent detection, thereby illustrating the need for different, more sensitive methods of arterial stiffness detection.

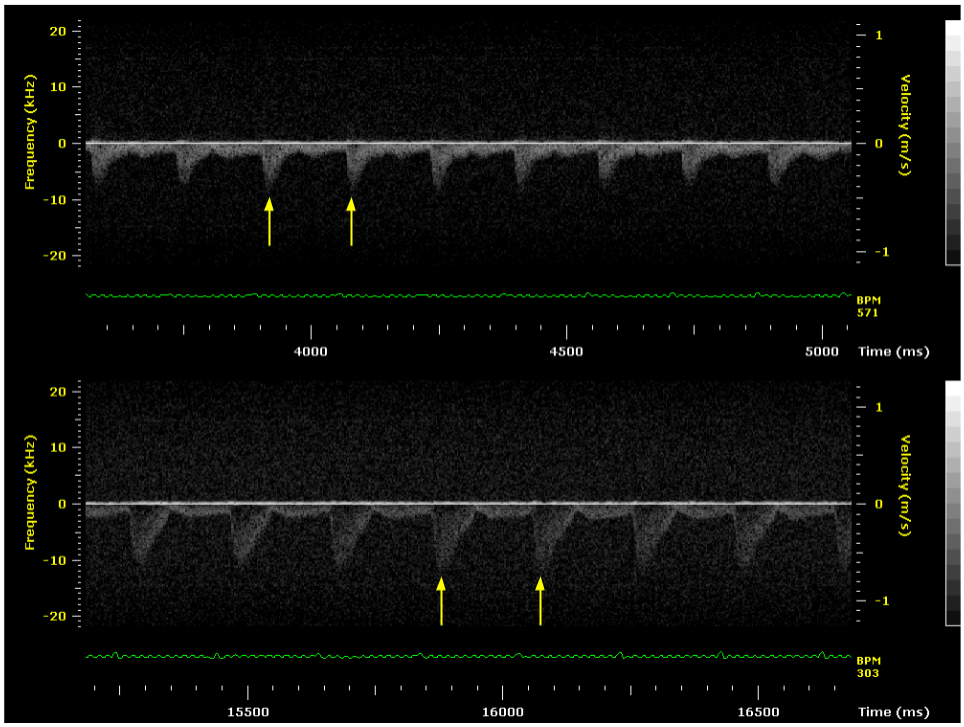

Figure 2.2: Representative pulsed wave doppler traces from the carotid arteries of a rat before entry into the experiment (top trace) versus after four weeks of no Vitamin D (bottom trace) in the diet. The yellow arrows show where the CA PSV is measured on the Doppler trace. The lower trace shows greater peaks in CA PSV compared to the top trace, indicating that CA PSV has increased with lack of Vitamin D, indicating arterial stiffening compared to the normal dietary level.

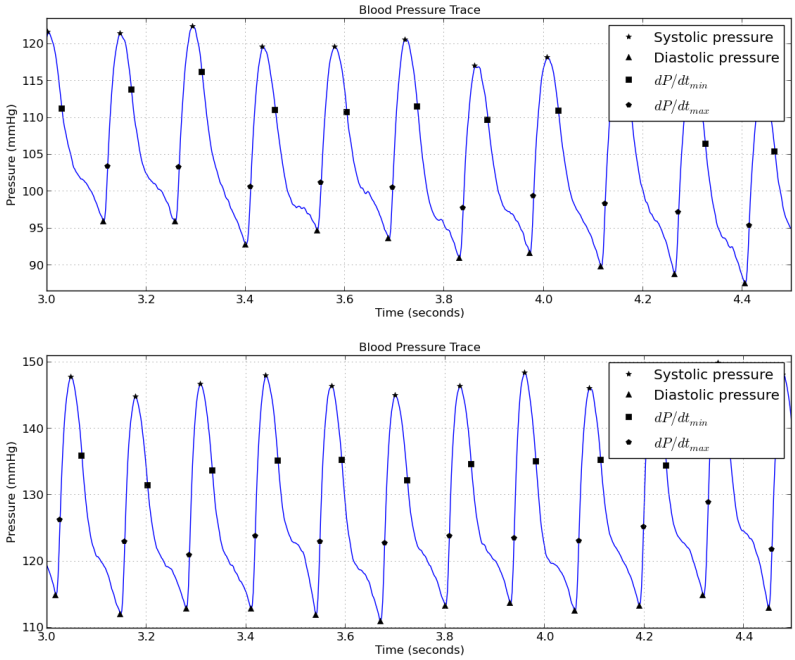

Figure 2.3: Sample data output using `PWanalyze` designed specifically for this experiment. The pulse waveform data was obtained from a rat with a telemetry blood pressure catheter placed in the iliac artery. The top trace is a rat before entry into the experiment and the bottom trace is the same rat after four weeks of no Vitamin D in the diet. The symbols indicate the points in each pulse where each of the analysis parameters were equal to the values calculated. The program then generates output which takes averages of the values within a selected area and reports mean values for each parameter.

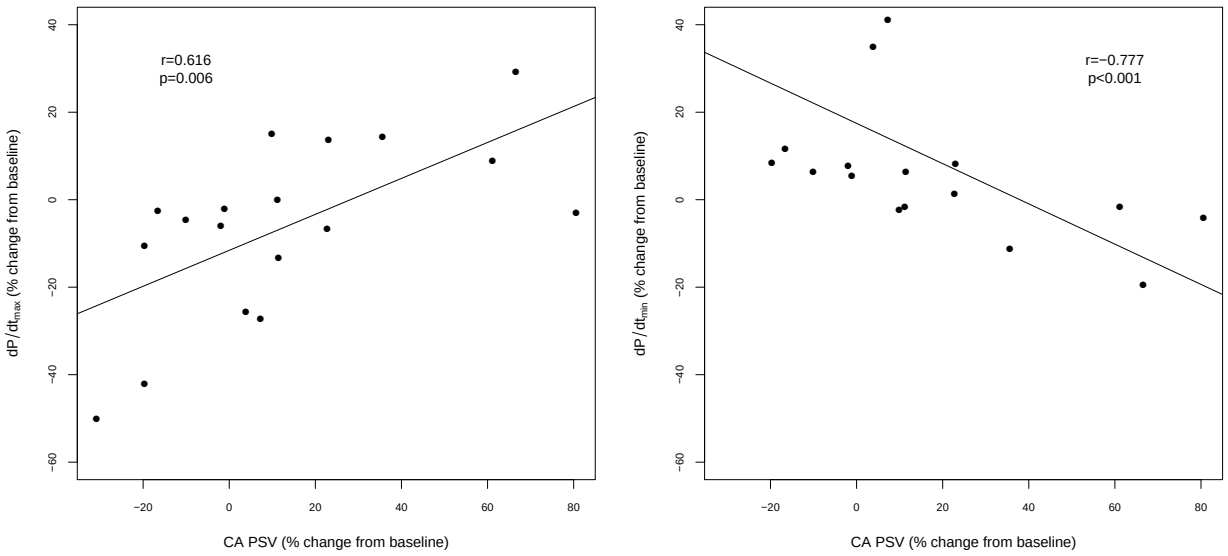

Figure 2.4: Correlation of carotid artery stiffness measured by carotid artery peak systolic velocity (CA PSV) with two different parameters calculated using custom-authored software created for this study, dP/dt_{max} and dP/dt_{min}. Two-tailed Spearmans statistics and p-values for the regression are shown. Data was expressed as a percent of the baseline (pre-diet treatment) values for each individual rat in order to remove inter-individual variation.

Values for dP/dt_{min} and dP/dt_{max} were calculated using `PWanalyze` and are shown for each treatment group at the end of the experiment in Table 2.2. Figure 2.3 shows two representative pulse waveform traces analyzed by `PWanalyze`. The tracings in Figure 2.3 show that dP/dt_{min} and dP/dt_{max} increased in magnitude at the end of the study for a rat in the 0 IU/g treatment group. The range of values for CA PSV was used to explore whether dP/dt_{min}, and dP/dt_{max} indicate arterial stiffness. The change in pulse waveform analysis parameters, dP/dt_{min}, and dP/dt_{max}, from baseline are both significantly correlated with the change in CA PSV (Figure 2.4; r =0.616, -0.777, respectively; $p < 0.01$ for both). The correlation is slightly stronger for dP/dt_{min} compared to dP/dt_{max}, which confirms that dP/dt_{min} is at least as good as dP/dt_{max} in detecting simlar changes as CA PSV, but we cannot say based on this analysis whether dP/dt_{min} is better or not despite the slightly higher r-value. The change in dP/dt_{min} and dP/dt_{max} did not vary significantly between treatment groups; see Table 2.2. Bland-Altman plots were generated as a second statistical method to support conclusions from the correlation analyses and to further examine the relationship between dP/dt_{min}, dP/dt_{max}, and CA PSV (Figure 2.5). The Bland-Altman plots showed similar systemic bias of dP/dt_{min} (-19%) and dP/dt_{max} (-24%) to underestimate the change arterial stiffness compared to CA PSV and low systemic bias when dP/dt_{min} was used to estimate dP/dt_{max} (-5%). The limits of agreement between dP/dt_{min} and CA PSV were the same as the limits of agreement between dP/dt_{max} and CA PSV (48%). This supports that dP/dt_{min} and dP/dt_{max} equally estimate the change in CA PSV and that CA PSV changes more than either dP/dt_{min} or dP/dt_{max} in response to arterial stiffness.

After developing the `PWanalyze` software using the chronic vitamin D dataset, we wanted to confirm whether this software could perform under different conditions where changes in arterial stiffness are expected. Specifically, we wanted to compare whether `PWanalyze` could detect acute changes in rats induced by vasodilatory and vasoconstrictive drugs in normal rats. Thus, this acute drug experiment was a separate data set used to confirm the results with dP/dt_{min} and dP/dt_{max}. Table 2.3 shows the effect of a saline vehicle, ACh, and NE on blood pressure, dP/dt_{min}, and dP/dt_{max}. The saline vehicle had no significant effect on systolic, diastolic, or pulse pressures, as well as having no effect on heart rate, and dP/dt_{max}. As expected, ACh caused a significant decrease in systolic blood pressure, diastolic blood

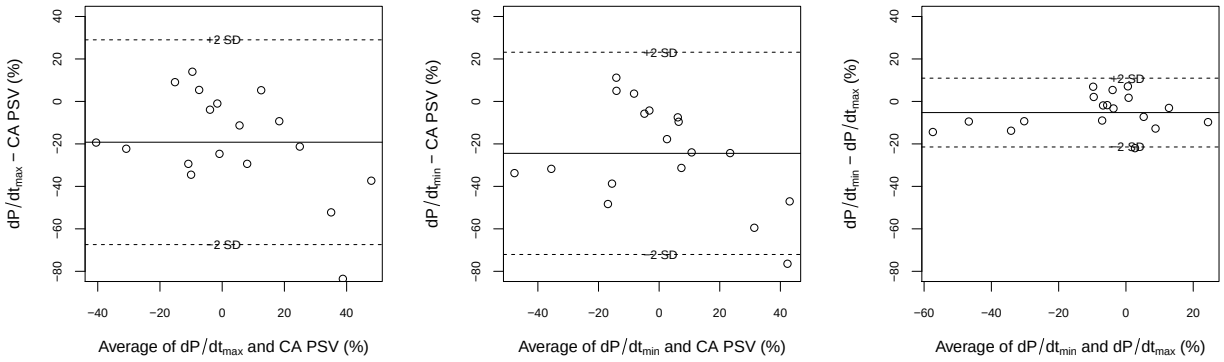

Figure 2.5: Bland-Altman plots comparing dP/dt_{max} (-19 ± 48%) and dP/dt_{min} (-24 ± 48%) to carotid artery stiffness measured by carotid artery peak systolic velocities (CA PSV), and dP/dt_{max} to dP/dt_{min} (-5 ± 16%). Data were expressed as a percent of the baseline (pre-diet treatment) values for each individual rat in order to remove inter-individual variation.

pressure, and pulse pressure, but no effect on heart rate. After ACh administration, both dP/dt_{min} and dP/dt_{max} significantly changed compared to the saline vehicle. The significant negative change in dP/dt_{max} is indicative of decreasing slope in the rapid systolic rise in pressure, consistent with decreased arterial stiffness. The positive change in dP/dt_{min} indicates a less steep downward slope in the rapid diastolic decrease in pressure with each pulse, consistent with decreased arterial stiffness. In contrast, NE administration significantly increased systolic, diastolic, and pulse pressures, but also showed a significant decrease in heart rate. The decrease in heart rate after NE confounds interpretation of arterial stiffness from systolic and especially pulse pressures. However, a drop in heart rate would tend to decrease, not increase pulse pressure, thus the observed increase in pulse pressure after NE administration can confidently be attributed to increased arterial stiffness. Similarly, the large significant positive change in dP/dt_{max} indicates a much steeper slope in the rapid systolic rise in pressure with each pulse, consistent with increased arterial stiffness. While heart rate changes by themselves can alter dP/dt_{max}, the observed decrease in heart rate would tend to reduce, not increase slope. Since we observed a positive change, this indicates the significant dP/dt_{max} increase is indicative of increased arterial stiffness. Finally, the dP/dt_{min} had a large negative change after NE administration compared to pre-injection (negative $\Delta dP/dt_{min}$), indicating

Table 2.3: Effect of a saline vehicle (0.5 mL/kg) and vasoactive drugs acetylcholine (ACh 0.91 ng/kg) and norepinephrine (NE 0.02 mg/kg) on blood pressure, dP/dt_{max}, and dP/dt_{min}. Values reported as median and range in parentheses. The saline vehicle is the control. Note: *, $p < 0.05$; **, $p < 0.01$ versus vehicle group in a posteriori Mann-Whitney U-tests with Bonferonni correction after Kruskal Wallis test.

	ΔSystolic Blood Pressure (mmHg)	ΔDiastolic Blood Pressure (mmHg)	ΔPP (mmHg)	ΔHR (bpm)	$\Delta dP/dt_{max}$ (mmHg/s)	$\Delta dP/dt_{min}$ (mmHg/s)
Vehicle	0	-1	0 (0-1)	-1	-2	2
n=4	(-3-6)	(-3-6)	(0-1)	(-4-6)	(-40-73)	(-39-12)
ACh	-16	-10	-5	3	-333	75
n=4	(-21- -12)*	(-16- -7)*	(-7- -4)*	(2-6)	(-398- -249)*	(69-88)*
NE	66	41	25	-13	1012	-1209
n=4	(63-80)*	(37-46)*	(23-33)*	(-14- -8)*	(499-1394)*	(-1645- -1037)*

a steeper negative slope in the rapid diastolic decrease in pressure with each pulse, consistent with increased arterial stiffness. It is known that dP/dt_{max} can increase when there is increased pulse pressure at a given heart rate [33]. Although dP/dt_{min} has not been previously used to measure arterial stiffness, changes in pulse pressure at a given heart rate could possibly affect dP/dt_{min}. However, changes in pulse pressure and heart rate did not account for all of the changes in dP/dt_{min} and dP/dt_{max} in this study. For example, in the 0 IU/g group dP/dt_{min} decreased further than what was predicted from the change in pulse pressure and heart rate and dP/dt_{max} increased further than what was predicted from the change in pulse pressure and heart rate.

2.4 Discussion

The primary discovery of this study shows dP/dt_{min} to be an equally good indicator of arterial stiffness in comparison to dP/dt_{max}through comparison with acute and chronic changes in arterial stiffness. The correlation and Bland-Altman comparison to CA PSV was similar for dP/dt_{min} and dP/dt_{max}. NE administration caused dP/dt_{min} to decrease significantly and dP/dt_{max} to increase significantly. ACh caused a negative change in dP/dt_{min} and a positive change in dP/dt_{max} but was not significant. The changes seen with NE and

ACh administration are consistent with the increase and decrease of arterial stiffness from vasoconstriction and vasodilation, respectively.

In practice, blood pressure telemetry and cardiovascular research software packages are necessary to calculate dP/dt_{min} and dP/dt_{max}. Many commercial software packages are able to calculate dP/dt_{max} from arterial blood pressure traces; they are also able to calculate dP/dt_{min} and dP/dt_{max} from pressure-volume loops in the heart. The `PWanalyze` software written for this experiment is the only known software package that calculates dP/dt_{min} from arterial blood pressure traces. Software support for dP/dt_{min}, dP/dt_{max}, systolic blood pressure, diastolic blood pressure, and pulse pressure in `PWanalyze` increases the sensitivity of detecting acute changes in the arterial wall. `PWanalyze` is beneficial in cardiovascular toxicology and pharmacology research for two reasons: (i) a high resolution rodent ultrasound machine to measure CA PSV is not required to calculate dP/dt_{min} and dP/dt_{max} and (ii) commercial software to calculate dP/dt_{max} is not needed. The resolution needed for rodent cardiovascular ultrasound is higher than any clinical machine is capable of measuring and the high resolution ultrasound needed is too expensive for all but the largest cardiovascular research groups to afford. `PWanalyze` is designed to allow greater access for all cardiovascular researchers with less expensive ultrasound machines. The commercial software that is available to calculate dP/dt_{max} is very expensive, therefore, free open source software could become an invaluable tool for researchers in this era of difficulty in obtaining research funds.

At the iliac artery, the dP/dt_{min} measured varied significantly between treatment groups, whereas the dP/dt_{max} measured did not vary significantly between treatment groups. Therefore, dP/dt_{min} should be examined in pulse waveform analyses. This new approach complements the pre-existing use of dP/dt_{max}. Examining both dP/dt_{min} and dP/dt_{max} is advantageous because observing similar trends between dP/dt_{min} and dP/dt_{max} provides more confidence in diagnosing arterial stiffness. A rodent telemetry system can be used to measure dP/dt_{min} and dP/dt_{max} to remove the cardiovascular depressant effect of anesthesia [33]. However, if a rodent telemetry system is not available, dP/dt_{min} and dP/dt_{max} can be measured under anesthesia in a terminal preparation with a heparinized fluid-filled catheter manometer system or a Millar catheter.

The drawback of using dP/dt_{min} and dP/dt_{max} in rodents is that dP/dt_{min} and dP/dt_{max} are

measured through invasive techniques requiring intravascular access. In humans, dP/dt_{max} has been measured by pulse applanation tonometry in the radial artery; however, this technique has not been reported in rats [4, 116]. To measure arterial stiffness in rats using dP/dt_{min}, the pressure catheter must be placed near the iliac artery because dP/dt_{min} has not been verified as a measure of arterial stiffness in other locations. For example, dP/dt_{min} might not be a measure of arterial stiffness in the aortic arch due to the effects of left ventricular relaxation [74, 138]. The relaxation of an artery (dP/dt_{min}) is a measure of the artery's stiffness. A stiff artery requires more force than an elastic artery when stretching to accommodate blood. At the same heart rate, this means that the higher pressure required by a stiffer artery will lead to a higher dP/dt_{max} value compared to a more compliant artery. Conversely, the increased force used to stretch the stiff artery causes the artery to recoil faster than the elastic artery leading to a decrease in dP/dt_{min}. Thus, the relaxation or elastic recoil of the artery is measured by dP/dt_{min} when the catheter is inserted into the iliac artery. In contrast, when the catheter is adjacent to the heart, dP/dt_{min} measures relaxation of the left ventricle [74, 138]. The iliac artery is sufficiently distant from the heart that the pressure difference from left ventricle relaxation is highly unlikely to affect dP/dt_{min}. Left ventricle contraction is measured by dP/dt_{max} when the catheter is adjacent to the heart [74, 138]. Arterial stiffness is measured by dP/dt_{max} in the iliac artery and radial artery [4]. Future work should address where dP/dt_{min} and dP/dt_{max} measure arterial stiffness in the arterial tree. The iliac artery is an easily accessible area to measure arterial stiffness in rodent cardiovascular studies. The iliac artery was used to obtain measures of arterial stiffness, dP/dt_{min} and dP/dt_{max}, that were valuable in detecting both chronic and acute changes in arterial stiffness.

Toxicology and pharmacology studies that measure intravascular blood pressure should use the parameters dP/dt_{min} and dP/dt_{max} to detect changes in arterial stiffness. The discovery of these new indicators of arterial stiffness increases the available measurements at the disposal of researchers. Development of `PWanalyze` software further decreases financial and technical barriers to cardiovascular researchers in obtaining valuable measurements of arterial stiffness. Using `PWanalyze` software, dP/dt_{min} and dP/dt_{max} can be easily calculated to increase the sensitivity of detecting acute changes in the vascular wall. With more accurate

measurement of arterial stiffness in rodent models of cardiovascular disease, translational cardiovascular studies will be better able to predict cardiovascular morbidity and mortality associated with arterial stiffness in humans.

Chapter 3

Wave Separation Analysis

This chapter is dedicated to outlining the mathematical approach taken in the Chapter 4 for wave separation analysis and how to calculate backward waves in rat peripheral arteries.

Wave separation analysis has been applied to the ascending aorta in the rat [17, 24, 43, 60, 105]. To perform wave separation analysis in the ascending aorta, a thoracotomy is performed so that a flow probe can be placed on the aorta. A pressure probe is then placed into the ascending aorta by insertion through the carotid artery. To place the flow probe in the ascending aorta, the rat must be endotracheally intubated and mechanically ventilated before the chest is opened. Intubation and mechanical ventilation are technically difficult to perform and affect the cardiopulmonary status of the rat. This thesis explores using peripheral arteries for wave separation analysis to increase the feasibility of this technique in more rodent cardiovascular studies. The advantage of using peripheral arteries for wave separation analysis is that it less technically demanding for the researcher and surgically invasive for the rodent. The objective of this chapter is to outline the mathematics behind a novel technique for wave separation analysis in rat peripheral arteries in more detail than is provided in Chapter 4.

3.1 Fourier Analysis

Fourier analysis was used in this thesis for wave separation analyses, and thus a brief discussion on the approach taken is needed here. Fourier analysis is a method of uniquely respresenting a waveform as a series of sinusoidal functions also known as harmonic waves. Representing the waveform as harmonic waves simplifies the study of blood pressure and flow. To perform wave separation analysis, the pressure and flow traces are represented in

the frequency domain using a Fourier series (Equations 3.1a and 3.1b; Appendix B).

$$P(t) = \sum_{n=1}^{k=\infty} M_{P,n} \cos(n\omega t + \varphi_{P,n}), \tag{3.1a}$$

$$Q(t) = \sum_{n=1}^{k=\infty} M_{Q,n} \cos(n\omega t + \varphi_{Q,n}), \tag{3.1b}$$

$$\omega = \frac{2\pi}{L}, \tag{3.1c}$$

where $t \in \mathbb{R}$ (i.e., time is in the set of real numbers), $P(t)$ is pressure measured in the artery, $Q(t)$ is flow measured in the artery, n is a harmonic number in the Fourier series, $M_{P,n}$ is the modulus of the nth harmonic of pressure, $M_{Q,n} \in \mathbb{R}$ is the modulus of the nth harmonic of flow, ω is the angular frequency, L is the period of the cardiac cycle, $\varphi_{P,n}$ is the phase angle at the nth hamonic of pressure, and $\varphi_{Q,n}$ is the phase angle at the nth harmonic of flow. Additionally, k is the number of harmonics used and is usually truncated at 15 to 20 harmonics in this type of analysis [80, 88]. Each harmonic is expressed in phasor notation, described in Appendix C.

The number of harmonics that can have physical meaning depends both on the sampling rate and accuracy of the recording equipment. If there are N time-points recorded in the pressure or flow measurement, $N/2$ harmonics can be meaningfully determined because each harmonic has two variables, modulus and phase angle. In this experiment, the sampling rate of 1000 samples per second limits the frequency that can be analyzed to 500 Hz. Because the rat's heart rate is generally less than 400 beats per a minute (6.7 Hz), there are a 150 data points for each heart beat and therefore 75 harmonics can be significant. Aliasing occurs when there are harmonics above $N/2$ that are are significant (have a non-trivial modulus). The recording equipment uses a 160 Hz filter for blood flow and an 1 kHz filter for blood pressure. Aliasing is technically possible with a 1kHz filter for blood pressure and a sampling rate of 1000 samples per a second; however, physiologically, the pressure waveforms have negligible power above 70Hz in the rat so significant aliasing is unlikely [80].

To compare with human wave separation analysis, generally ten harmonics (up to 30 Hz) are calculated in humans and ten to fifteen harmonics (up to 100 Hz) have been calculated previously in rats [88, 80]. To quantitatively determine the significant harmonic terms in the arterial waveform, the total variance of the original measured wave values V_t (Equation 3.2)

can be compared against the variance of the calculated Fourier series V_s (Equation 3.3) using Parseval's theorem [86]. Parseval's theorem states that the variance of the original function is equal to the variance of the Fourier series.

$$V_t = \frac{1}{m}\sum_{t=1}^{m} P(t)^2 - \left(\frac{1}{m}\sum_{t=1}^{m} P(t)\right)^2, \tag{3.2}$$

$$V_s = \frac{1}{2}\sum_{n=1}^{k} M_{P,n}^2, \tag{3.3}$$

where m is the number of ordinates and k is the number of harmonics. Often, $\frac{V_s}{V_t}$ exceeds 0.995 in seven or eight harmonics [88]. For the purposes of this thesis, the Fourier series is considered sufficiently accurate when $\frac{V_s}{V_t} > 0.99$. The Fourier series was found to be sufficiently accurate in this thesis work at five harmonics and to exceed 99.5% accuracy at thirteen harmonics in a preliminary experiment with twenty male Wistar Rats.

3.2 Impedance

In the arterial system, impedance is the ratio of oscillatory pressure to flow [88]. The concept of impedance is borrowed from electrical engineering and is analagous to the ratio of voltage to alternating current in a circuit. Impedance is based on Ohm's law for alternating current; that is, the relationship between current and voltage in a circuit is described by a complex quantity called impedance. When the pressure and flow (analagous to voltage and current) are steady, impedance is more commonly known as resistance. Two types of impedance, *input impedance* Z_{in} and *characteristic impedance* Z_c, are calculated in wave separation analysis [106, 133]; they are defined in the subsequent sections.

3.2.1 Input Impedance

Input impedance (Z_{in}) is defined as the ratio of oscillating pressure and oscillating flow at a particular arterial site [88]. Input impedance is calculated by

$$Z_{in}(t) = \sum_{n=1}^{k} \frac{M_{P,n}\cos(\pi\omega t + \varphi_{P,n})}{M_{Q,n}\cos(\pi\omega t + \varphi_{Q,n})}, \tag{3.4a}$$

$$M_{Z_{in},n} = \frac{M_{P,n}}{M_{Q,n}}, \tag{3.4b}$$

$$\varphi_{Z_{in},n} = \varphi_{P,n} - \varphi_{Q,n}, \tag{3.4c}$$

$$Z_{in}(t) = \sum_{n=1}^{k} M_{Z_{in},n}\cos(\pi\omega t + \varphi_{Z_{in},n}), \tag{3.4d}$$

where $t \in \mathbb{R}$, n is a harmonic number, k is the total number of harmonics computed, $M_{Z_{in},n}$ is the modulus of the nth harmonic of input impedance, ω the angular frequency is defined in Equation 3.1c, and $\varphi_{Z_{in},n}$ is the phase angle at the nth harmonic of impedance. Input impedance includes both forward and backward travelling waves [133]. The presence of backward travelling waves introduces a phase shift between the measured pressure and flow waves. Input impedance is a complex number due to this phase shift (Equation 3.4d). Phasor arithmetic is used to divide the Fourier harmonics of pressure and flow (Equation 3.4b and 3.4c). Phasor arithmetic is outlined in Appendix C.

3.2.2 Characteristic Impedance

Characteristic impedance (Z_c) is the ratio between oscillatory pressure and flow in an artery, when the waves are not influenced by wave reflection [88]; i.e., only forward travelling waves are considered. Obtaining Z_c from experimental data is not possible because there is no circumstance where pressure and flow are not altered by wave reflection; however, Z_c can be estimated from Z_{in} [88]. When estimating characteristic impedance, only the moduli of the input impedance are considered. The phase is set to zero because there are no wave reflections by definition of characteristic impedance. Therefore, characteristic impedance is a real number because there is no phase shift. In the absence of wave reflections, the pressure would travel in phase with the flow. There are many methods to estimate the characteristic

impedance from the input impedance. Mitchell et al. [80] found the three most common methods of calculating Z_c to be equivalent in rats: Z_c computed as the average of moduli of Z_{in} above and including the second harmonic, Z_c computed as the average of all moduli after and including the first input impedance moduli minimum, and Z_c computed as the average of all moduli after the first input impedance moduli minimum. For this experiment, Z_c was computed as the average of moduli of Z_{in} above and including the second harmonic,

$$Z_c = \frac{1}{k-1}\sum_{n=2}^{k} M_{Z_{in},n}, \tag{3.5}$$

where $Z_c \in \mathbb{R}$ is the characteristic impedance, $M_{Z_{in},n}$ is the modulus of input impedance at the nth harmonic and k is the maximum amount of harmonics calculated. In humans, Z_c average was calculated above 2 Hz (the second harmonic) [85]. In rats, the average has been computed from the second to tenth harmonic [80]. In another human studies, Z_c is the average of the third to the tenth harmonic and of the fourth to the tenth harmonic [106, 135]. The Z_c average was chosen to be from the second to the tenth harmonic for this thesis.

3.3 Backward Wave Separation

The forward and backward pressure waves can be calculated from the measured pressure and flow waves once characteristic impedance is known. The Fourier series representing the forward and backward pressure waves are calculated from the Fourier series of the measured pressure and flow waves follows [135]:

$$P_f = Z_c Q_f = \frac{P_m + Z_c Q_m}{2}, \tag{3.6}$$

$$P_b = -Z_c Q_b = \frac{P_m - Z_c Q_m}{2}, \tag{3.7}$$

where Equations 3.6 and 3.7 hold for each harmonic of the forward pressure wave P_f, forward flow wave Q_f, backward pressure wave P_b, backward flow wave Q_b, measured pressure wave P_m, and measured flow wave Q_m.

Equations 3.6 and 3.7 can be expanded and simplified using phasor arithmetic outlined in Appendix C:

$$P_f(t) = \frac{1}{2}\sum_{n=1}^{k}\Big[M_{P_m,n}\cos(\pi\omega t + \varphi_{P_m,n}) + Z_c M_{Q_m,n}\cos(\pi\omega t + \varphi_{Q_m,n})\Big], \tag{3.8}$$

where $t \in \mathbb{R}$, n is a harmonic number in the Fourier series, i is the imaginary unit, $P_f(t)$ is forward travelling pressure in the artery, Z_c is the characteristic impedance of the artery, ω the angular frequency is defined in Equation 3.1c, $M_{P_m,n}$ is the modulus of the nth harmonic of measured pressure, $\varphi_{P_m,n}$ is the phase angle at the nth harmonic of measured pressure, $M_{Q_m,n}$ is the modulus of the nth harmonic of measured flow, and $\varphi_{Q_m,n}$ is the phase angle at the nth harmonic of measured flow.

The addition of the harmonic cosine functions are then represented using complex numbers in rectangular form for each harmonic n:

$$
\begin{aligned}
a_{P,n} &= M_{P_m,n}\cos(\varphi_{P_m,n}),\\
a_{Q,n} &= Z_c M_{Q_m,n}\cos(\varphi_{Q_m,n}),\\
b_{P,n} &= M_{P_m,n}\sin(\varphi_{P_m,n}),\\
b_{Q,n} &= Z_c M_{Q_m,n}\sin(\varphi_{Q_m,n}),\\
a_n &= a_{P,n} + a_{Q,n},\\
b_n &= b_{P,n} + b_{Q,n}.
\end{aligned}
$$

The rectangular form is converted back into a harmonic cosine function of the forward pressure wave:

$$
\begin{aligned}
M_n &= \sqrt{a_n^2 + b_n^2},\\
\varphi_n &= \arctan(\frac{b_n}{a_n}),\\
P_f(t) &= \frac{1}{2}\sum_{n=1}^{k}[M_n\cos(\pi\omega t + \varphi_n)].
\end{aligned}
$$

The subtraction of harmonic cosine functions is also represented using complex numbers in

rectangular form for calculation of the backward pressure wave:

$$P_b(t) = \frac{1}{2}\sum_{n=1}^{k}\Big[M_{P_m,n}\cos(\pi\omega t + \varphi_{P_m,n}) - Z_c M_{Q_m,n}\cos(\pi\omega t + \varphi_{Q_m,n})\Big], \tag{3.9}$$

$$a_{P,n} = M_{P_m,n}\cos(\varphi_{P_m,n}), \tag{3.10}$$

$$a_{Q,n} = Z_c M_{Q_m,n}\cos(\varphi_{Q_m,n}), \tag{3.11}$$

$$b_{P,n} = M_{P_m,n}\sin(\varphi_{P_m,n}), \tag{3.12}$$

$$b_{Q,n} = Z_c M_{Q_m,n}\sin(\varphi_{Q_m,n}), \tag{3.13}$$

$$a_n = a_{P,n} + a_{Q,n},$$

$$b_n = b_{P,n} + b_{Q,n},$$

$$M_n = \sqrt{a_n^2 + b_n^2},$$

$$\varphi_n = \arctan(\frac{b_n}{a_n}),$$

$$P_b(t) = \frac{1}{2}\sum_{n=1}^{k}[M_n\cos(\pi\omega t + \varphi_n)],$$

where $P_b(t)$ is backward travelling pressure in the artery.

3.4 Wave Separation Analysis Parameters

After performing wave separation analysis, reflection index, characteristic impedance, amplitude of the forward pressure wave, and amplitude of the backward pressure wave can be calculated as potential measures of arterial stiffness.

The reflection index RI represents the ratio of the backward wave to the measured wave and is calculated by:

$$RI = \frac{A_b}{A_f + A_b}$$

where A_b is the amplitude of the backward travelling pressure wave $P_b(t)$, and A_f is the amplitude of the forward travelling pressure wave $P_f(t)$.

3.5 Assumptions in Wave Separation Analysis

Wave separation analysis assumes that the arterial system can be treated as a simple linear model [29, 88]. In practice, each individual harmonic term of pressure is related only to the corresponding harmonic term of flow [88]. The effect of interaction, introduced by current blood pressure and flow measurement techniques, between harmonic terms is small, less than one percent, and can therefore be neglected [29, 88].

3.6 Software Development

The `WSanalyze` software package was developed using Python 2.7, a high-level interpreted language that is commonly used in many scientific communities [122]. `WSanalyze` uses several widely distributed packages including Numerical Python for ease of mathematical operations, OpenGL for display of data and results, and GLUT for a simple window interface [5, 56, 109]. The purpose of developing software was to provide researchers without any programming ability a tool to perform wave separation analysis in rats. The user of `WSanalyze` is able to specify a data file to be analyzed. The data are displayed graphically, and the user can view the blood pressure and blood flow at any time point in the data file. The desired time points to be analyzed can then be selected by the user. The results of wave separation analysis are displayed graphically and are output as a text file for use in further statistical analysis.

When a data file is read by `WSanalyze`, the flow and pressure data are aligned for any phase shift errors introduced by catheter and flow probe placement. The maximum first derivative of the upstroke of the pressure and flow tracings are used to align the pressure and flow data. The aligned data are then displayed to the user. Then once the user selects an area of the data to be analyzed, a peak detection algorithm is used to detect the pulses to be analyzed. Analysis involves first converting the pressure and flow tracing for each pulse into a Fourier series by the method in Appendix B. Simpson's rule is used for numerical integration when calculating the coefficients of the Fourier series in Equations B.2, B.3, and B.4. Input impedance is then calculated by Equation 3.4a and is used in the calculation of characteristic impedance by Equation 3.5. Once characteristic impedance is known, the pressure wave can

be separated into forward and backward waves by Equations 3.8 and 3.9. Wave separation analysis parameters, reflection index, characteristic impedance, amplitude of the forward pressure wave, and amplitude of the backward pressure wave are then calculated for each pulse in the selection to be analyzed. The wave separation analysis parameters reported by `WSanalyze` are an average of the values calculated for the selection of pulses specified by the user.

To verify that the Fourier series calculations were correct, test data based on known functions were generated then visual inspection of the Fourier transform and comparison of variance between the Fourier series and original function were performed. The wave separation analysis algorithm was confirmed by inputting pressure and flow tracings from a canine ascending aorta and comparing the results to those of Westerhof et al. [133]. Figure 3.1 shows the similarity between the forward and backward pressure waves calculated by `WSanalyze` and the forward and backward waves calculated by Westerhof et al. [133]. Verifying the `WSanalyze` software against a known reference solution, the data of Westerhof et al., is a necessary step to confirm program correctness prior to using the wave separation analysis algorithm against experimental data. Chapter 4 presents the next step for validation, two separate groups of rats were used to test the `WSanalyze` software. The first group was used to develop the surgical data collection technique and confirm that `WSanalyze` software can be used on rat pulse waveforms. The second group of normal Wistar rats was subjected to acute vasoactive drug injections to confirm that the wave separation analysis parameters are meaningful measures of arterial stiffness in rats.

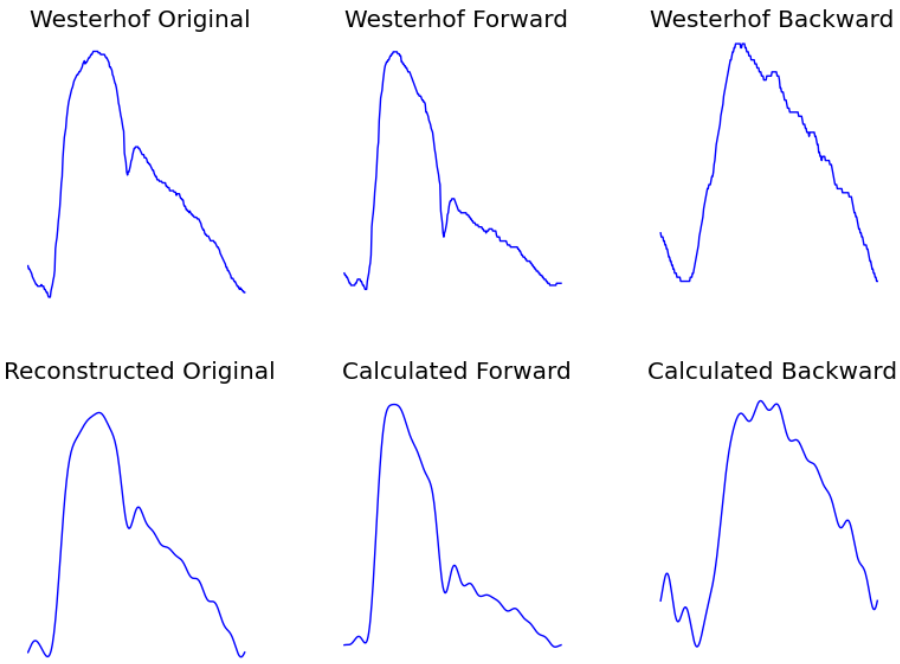

Figure 3.1: Validating `WSanalyze` software against a known data set. Canine ascending aorta pressure (Westerhof Original) and flow (not shown) tracings from Westerhof et al. were used to are a dataset to test the `WSanalyze` software [133]. The waves presented in the above figure are not on the same vertical scale. Generally, the backward wave is smaller than the corresponding forward wave. The original forward and backward pressure waves (top row) presented in the landmark paper of Westerhof et al. are matched by the calculated forward and backward pressure waves (bottom row) from `WSanalyze`. The reconstructed measured pressure wave (bottom row) is from the sum of the calculated forward and backward pressure waves.

Chapter 4

Wave Separation Analysis in Blood Pressure Measured at the Femoral Artery of Rats

4.1 Preamble

The following study will be submitted to the Journal of Pharmacological and Toxicological Methods. Replication of some material from the introduction is unavoidable. This chapter describes a new technique of applying wave separation analysis to the femoral artery to detect acute changes in the stiffness of the rat arterial wall. I contributed 90% of the manuscript. I developed the software, performed the experiments, analyzed the data, prepared figures, and drafted the manuscript. Lynn P. Weber and I designed the research study, interpreted results of experiments, and edited and revised the final version of this manuscript.

4.2 Introduction

Arterial hypertension measured using indirect (cuff) techniques at the brachial artery has long been known to be a major cardiovascular risk factor in humans [8]. However, end-organ damage is also more closely related to central arterial blood pressure than brachial arterial blood pressure; hypertension management is more effective when based on central arterial blood pressure than peripheral arterial pressure [108]. In addition to the difficulty measuring central pressure directly, a major issue is that brachial arterial blood pressure varies widely from central arterial blood pressure due to the pulse pressure amplification phenomenon [70]. The pulse pressure amplification phenomenon can be explained by wave reflections [93]. A pressure wave is generated for each heart beat that travels down the artery called the

incident or forward pressure wave. When the forward pressure wave reaches a branching or narrowing in the artery, a portion of the wave is reflected back and is then called a backward pressure wave. The backward wave reaches peripheral arteries, such as the brachial artery, earlier than the central arteries. Therefore the peripheral backward pressure wave sums with the forward pressure wave in systole rather than diastole leading to the pulse pressure amplification. The relationship between the forward pressure wave and the backward pressure wave has been shown to be a better indicator of arterial stiffness than brachial cuff blood pressure [130]. An increase in the amplitude of backward pressure waves has been found to be a consistent predictor of cardiovascular mortality independent of brachial arterial blood pressure [129, 130]. Recent consensus has found that wave reflections and central arterial hemodynamics are an early and sensitive predictor of cardiovascular morbidity and mortality and can be used to guide pharmacological therapy [127].

The rat is an important model for cardiovascular disease and pharmacological development. Wave reflections have been assessed in rats for varying pathophysiological states such as aging, left ventricular hypertrophy, hypertension, calcification of arteries, chronic renal failure, and diabetes [18, 16, 20, 24, 105]. Wave separation analysis in rats has been based on ascending aorta pressure and flow measurements [16, 24, 43, 60, 105]. To measure flow in the aorta, a thoracotomy needs to be performed. The rat must then undergo endo-tracheal intubation and mechanical ventilation once the chest cavity is opened. However, mechanical ventilation effects the cardiopulmonary status of the rat and requires specialized equipment and training, thereby limiting the physiological relevance and wide applicability of this approach. The goal of this study is to explore novel approaches for wave separation analysis that do not require a thoracotomy and mechanical ventilation, allowing for more physiological measurements and greater potential for a wider number of researchers to use these less invasive techniques.

Traditional measurements of arterial stiffness other than systolic blood pressure and pulse pressure include carotid peak systolic velocity (CA PSV), pulse wave velocity, and transit-time of the arterial pulse (TT). CA PSV is commonly used to indicate carotid artery stenosis [36]. CA PSV is also used as an indicator of arterial stiffness because arterial stiffening causes a stenotic-like condition. Transit-time can be used to as an estimate of pulse wave

velocity. Pulse wave velocity is a standard arterial stiffness measurement in humans and has been shown to precede hypertension and structural changes to the arterial wall in rats [70, 41]. Transit-time can be measured non-invasively at the same time as CA PSV; this is an advantage over only measuring pulse wave velocity in this experiment.

This study aims to present a method of wave separation analysis in a peripheral artery where characteristic impedance, backward wave amplitude, and reflection index characterize the arterial system of a rat. Two sites were examined for suitability and ease of use for peripheral wave separation analysis: the femoral artery and the carotid artery. After an initial exploratory experiment, the femoral artery was selected for further evaluation using acutely administered drugs to induce vasodilation and vasoconstriction to test how well the wave separation analysis software performed. Wave separation analysis parameters were compared with traditional indicators of arterial stiffness: blood pressure, CA PSV, and TT. The goal was to validate that backward waves could be measured at a peripheral artery in the rat and prove that wave separation analysis parameters measured arterial stiffness in the peripheral arterial system of rats. Backward wave amplitude was found to be a sensitive indicator of arterial stiffness suitable for detecting acute changes to the vasculature.

4.3 Methods

4.3.1 Study Animals and Care

This work was approved by the University of Saskatchewan Animal Research Ethics Board and adhered to the Canadian Council on Animal Care guidelines for human use. Eleven male Wistar rats ranging in weight from 425 to 594 grams were used in Experiment 1 for development of the surgical model and analysis software. Ten male Wistar rats ranging in weight from 404 to 505 grams were used in Experiment 2 for an acute vasoactive drug injection experiment. All rats were provided food and water ad libitum. The rats in Experiment 1 were housed in groups of two or three and the rats in Experiment 2 were housed individually. All rats were allowed to acclimatize two weeks before the start of the experiment. All rats were euthanized with Pentobarbital sodium (20 mL per 45 kg i.v.; Euthanyl; Bimeda-MTC

Inc., Cambridge, ON, Canada) while anesthetized after the experiment concluded.

4.3.2 Experiment 1: Model Development

Carotid and femoral blood pressure and blood flow measurements were performed in a terminal hemodynamic measurement procedure in eleven Wistar rats (425 to 594 grams) to develop a technique of applying wave separation analysis in the peripheral arteries. Calibration of the pressure transducer 1.4 Fr. Millar Catheter (ADInstruments, Colarado Springs, CO, USA) were performed with a mercury manometer, prior to the start of each experiment. Atmospheric zeros were recorded prior to insertion of the probe. Calibration of Labchart 8 (ADInstruments, Colarado Springs, CO, USA) to record flow data was confirmed against the TS420 Perivascular Flow Module (ADInstruments, Colarado Springs, CO, USA). The transducer and flow probe were kept in a saline bath prior to insertion. Rats were premedicated with Hydromorphone (20 microg/kg s.c.; Sandoz Canada Inc., Qc, Canada), then surgical anesthesia was induced with 5% isoflurane and 1 L/min of oxygen and maintained at 2% isoflurane and 0.5 L/min of oxygen. The left and right femoral arteries were dissected away from the femoral vein and nerve. A loose ligature using 5-0 braided silk suture was applied proximally on the left femoral artery to control blood flow during pressure catheter placement (Fine Science Tools Inc., BC, Canada). A tight ligature using 5-0 braided silk suture was placed distally to the catheter introduction site to increase the lumen size of the artery prior to insertion of the pressure catheter. A 22 guage one inch needle with the bevel bent backwards at a 45 degree angle (BD Insyte; Abbott Laboratories, North Chicago, IL, USA) was used to puncture the left femoral artery to introduce a 1.4Fr Millar Catheter (ADInstruments, Colarado Springs, CO, USA) that was then advanced three-quarters of an inch proximally. The loose ligature was then tightened and secured around the Millar catheter. A Transonics 1.5 PS flow probe was placed around the right femoral artery (ADInstruments, Colarado Springs, CO, USA). ECG was recorded continuously throughout the experiment. Blood pressure, blood flow, and the ECG were recorded continuously at a rate of 1000 samples per a second throughout the experiment using Labchart 8. Flow was recorded with a 150 Hz filter setting. In the rats used in the model development experiment, a fifteen minute recording was taken of femoral artery blood pressure and blood flow. Then the right and left

carotid arteries were isolated. The Millar catheter was placed into the right carotid artery using the same ligature technique as the femoral artery and a 22 guage one inch needle as a catheter introducer. Flow was measured with the Transonics flow probe placed on the left carotid artery. Measurements for wave separation analysis were taken ten minutes after instrumentation to allow the artery to relax after surgical manipulation. The location of measurements taken in the rats used for model development is shown in Figure 4.1.

4.3.3 Experiment 2: Vasoactive Drug Injection

The ten Wistar rats (404-505 grams) were subjected to a pulsed wave Doppler procedure, rested for seven days, and then hemodynamic measurements were performed in a terminal hemodynamic measurement procedure. During the pulsed wave Doppler procedure, a 25 gauge three-quarter inch butterfly catheter was successfully placed in the tail vein in four of the rats (Terumo Corporation, Tokyo, Japan). Saline (1 mL/kg) was injected intravenously through the tail vein catheter. Norepinephrine (0.02 mg/kg; [101]) was injected, followed by Sodium Nitroprusside (0.05 mg/kg; [120]). Between each injection, a washout period of five minutes was observed. Pulsed wave Doppler velocity was measured 30 seconds after each bolus drug injection which corresponded to the average time when blood pressure changed in preliminary experiments. Femoral blood pressure and flow were recorded in a terminal hemodynamic measurement procedure as described for Experiment 1 and shown in Figure 4.1. During the hemodynamic measurement procedure, a 26 gauge three-quarter inch over-the-needle catheter (BD Insyte; Abbott Laboratories, North Chicago, IL, USA) was placed in left femoral vein for bolus drug injections. The vasoactive drug experiment began ten minutes after instrumentation to allow the arteries to relax after surgical manipulation. The rats were subjected to the same bolus drug regime with saline, norepinephrine, and sodium nitroprusside injected intravenously with five minutes washout between injections. Ten waveforms, representing one respiration cycle, taken 30 seconds after each bolus drug injection were used for wave separation analysis and blood pressure.

4.3.4 Pulsed wave Doppler procedure

Pulsed wave Doppler ultrasound at the carotid artery was performed to obtain CA PSV, using a Vevo 3100 high frequency ultrasound (FujiFilm VisualSonics Inc., Toronto, ON, Canada). Each ultrasound procedure took no longer than 30 minutes for each animal. Prior to the ultrasound experiments, rats were premedicated with Hydromorphone (20 microg/kg s.c.; Sandoz Canada Inc., Qc, Canada), then surgical anesthesia was induced with 5% isoflurane and 1 L/min of oxygen and maintained at 2% isoflurane and 0.5 L/min of oxygen (Abbott Laboratories, Saint-Laurent, QC). Once anaesthetized, the rats were placed ventral side up on an electrocardiogram (ECG) plate (FujiFilm VisualSonics Inc., Toronto, ON, Canada) with each paw covered with electrode cream (Signa Crme, Parker Laboratories, Fairfield, NJ) and secured to ECG contacts with surgical tape to monitor HR throughout the entire experiment. A heated platform controlled by a temperature probe was inserted rectally to maintain internal body temperature at 37^{o}C. In order to prevent ultrasound artifacts, hair was removed by depilatory cream treatment (Nair, New York, NY, USA) application for two minutes, followed by physical removal with firm wiping with a series of dry tissues. EcoGel 200 (Eco-Med Pharmaceuticals, ON, Canada) was then applied to the thorax for ultrasound. A MX400 scanhead (FujiFilm VisualSonics Inc., Toronto, ON, Canada) was used to first locate the right carotid artery at the level of its bifurcation in B-mode and then pulsed wave Doppler traces were obtained 30 seconds after each injection of saline, norepinephrine and sodium nitroprusside. The CA PSV was calculated from the average peak velocity of 3 peaks. The transit-time (TT) between ventricular contraction denoted by the ECG-R wave and doppler upstroke was also calculated for 3 peaks. The averaged CA PSV and TT was then used per rat per injection in subsequent statistical analyses.

4.3.5 Wave Separation Analysis

The blood pressure data and blood flow data were analyzed using custom software written specifically for these experiments (`WSanalyze` software). For each calculation, the first ten consecutive cardiac cycles representing one respiratory cycle was selected for analysis. The pressure and flow waveforms were programmatically aligned to correct any spatial time delay

and filter-induced delay. The foot of the pressure waveform was aligned to the flow waveform by the first maximum derivative during systole [80]. The pressure and flow waves were represented as Fourier series as follows:

$$P(t) = \sum_{n=1}^{k} M_{P,n} \cos(n\omega t + \varphi_{Q,n}),$$
$$Q(t) = \sum_{n=1}^{k} M_{Q,n} \cos(n\omega t + \varphi_{Q,n}),$$
$$\omega = \frac{2\pi}{L},$$

where $t \in \mathbb{R}$, $P(t)$ is pressure measured in the artery, $Q(t)$ is flow measured in the artery, n is a harmonic number in the Fourier series, $M_{P,n}$ is the modulus of the nth harmonic of pressure, $M_{Q,n} \in \mathbb{R}$ is the modulus of the nth of flow, ω is the angular frequency, L is the period of the cardiac cycle, $\varphi_{P,n}$ is the phase angle at the nth harmonic of pressure, and $\varphi_{Q,n}$ is the phase angle at the nth harmonic of flow. Coefficients of the Fourier series of pressure and flow were calculated for the mean term through the 20th harmonic. The 2nd to the 10th harmonic were used in characteristic impedance calculation, whereas all 20 harmonics were used for calculations of forward and backward travelling waves. Arterial input resistance, the steady-flow term of the impedance spectrum, is calculated as mean pressure divided by mean flow. The arterial input impedance moduli are calculated for all 20 harmonics by dividing the pressure modulus by the flow modulus at each harmonic. The arterial input impedance phase for each harmonic is obtained by subtraction of flow phase by pressure phase for all 20 harmonics. The characteristic impedance, Z_c, was calculated by averaging all input impedance moduli from the 2nd to 10th harmonic. The characteristic impedance was then used to calculate the forward and backward waves by:

$$P_f(t) = \frac{1}{2} \sum_{n=1}^{k} \left[M_{P_m,n} \cos(\pi\omega x + \varphi_{P_m,n}) + Z_c M_{Q_m,n} \cos(\pi\omega x + \varphi_{Q_m,n}) \right]$$
$$P_b(t) = \frac{1}{2} \sum_{n=1}^{k} \left[M_{P_m,n} \cos(\pi\omega x + \varphi_{P_m,n}) - Z_c M_{Q_m,n} \cos(\pi\omega x + \varphi_{Q_m,n}) \right]$$

where $P_f(t)$ is forward travelling pressure in the artery, $P_b(t)$ is backward traveling pressure in the artery, Z_c is the characteristic impedance of the artery, $M_{P_m,n}$ is the modulus of the

nth harmonic of measured pressure, $\varphi_{P_m,n}$ is the phase angle at the nth harmonic of measured pressure, $M_{Q_m,n}$ is the modulus of the nth harmonic of measured flow, and $\varphi_{Q_m,n}$ is the phase angle at the nth harmonic of measured flow [135]. The systolic pressure, diastolic pressure, pulse pressure, forward pressure wave amplitude, backward pressure wave amplitudes, reflection index, and characteristic impedance were calculated for each cardiac cycle separately then the final values were averaged for each of the cycles analyzed and were then used per rat per injection treatment in subsequent statistical analysis.

4.3.6 Statistical Analysis

All baseline measurements are reported as a mean and standard error of all rats in the experiment. Data were tested with a Shapiro Wilk test for normal distribution. Comparison between femoral and carotid values ($n = 11$) for systolic pressure, diastolic pressure, pulse pressure, forward pressure wave amplitude, backward pressure wave amplitudes, reflection index, characteristic impedance, and CA PSV were performed with paired t-tests. Comparisons between treatments to measure vasoactive drug effects were calculated using a one-way ANOVA with repeated measures ($n = 10$). One-way ANOVA was followed by Dunnett's a posteriori tests to compare treatment effects, the saline treatment served as a control. Statistics were performed using SPSS Statistics Version 20 (IBM Canada Ltd., Markham, ON, Canada). Results with $p < 0.05$ (two-tailed) were considered to be statistically significant.

4.3.7 Peripheral Artery Site Selection

The femoral artery was chosen for further analysis in the acute vasoactive drug injection experiment because of ease of surgical manipulation and access to the femoral vein for drug injection. Complications in separate preliminary experiments included destruction of the artery during catheterization, catheter sliding out of the artery due to improper fastening, and hemorrhage. To avoid these complications, a small suture guage, such as 5-0 silk suture is recommended for fastening the arterial pressure catheter. Irregular breathing was observed after surgical instrumentation at the carotid artery in two rats due to phrenic nerve

stimulation. Using the femoral artery avoids complications associated with phrenic nerve stimulation. Characteristic impedance varied significantly between the carotid and femoral arteries (1000 ± 90 dynes sec cm^{-5}, 2940 ± 410 dynes sec cm^{-5}, respectively). It is important to note that impedance is site dependent; these reported values can be used as a reference point for future studies where impedance is measured in the carotid and femoral arteries of rats. Systolic blood pressure, diastolic blood pressure, pulse pressure, amplitude of the forward wave, amplitude of the backward wave, and reflection index did not vary significantly between the carotid and femoral arteries. Therefore, both the carotid and the femoral artery are suitable sites for a wave separation analysis study. The femoral artery was used for the acute vasoactive drug injection wave separation analysis study because of decreased surgical complications and ease of manipulation of the artery.

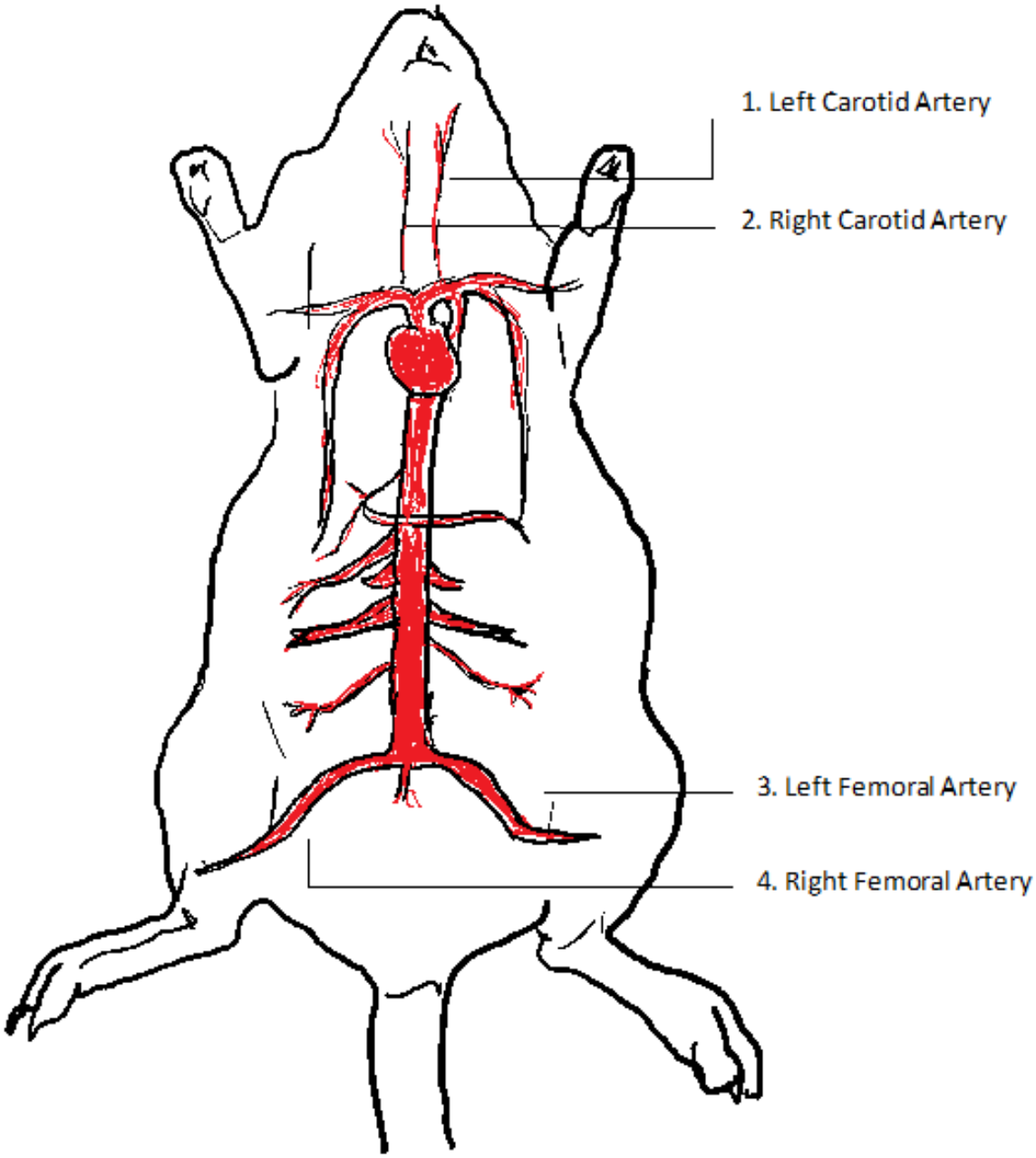

Figure 4.1: Diagram of arterial measurement sites for wave separation analysis. During model development in Experiment 1 the blood pressure was measured in the left femoral artery (3) and the blood flow was measured in the right femoral artery (4) simultaneously for 15 minutes. Then the blood pressure was measured in the left carotid artery (1) and the blood flow was measured in the right carotid artery (2) simultaneously for 15 minutes. During Experiment 2, the acute vasoactive drug experiment, bolus drug injections began five minutes after commencing blood pressure measurements in the left femoral artery (3) and blood flow measurements in the right femoral artery (4).

4.4 Results

The characteristic impedance of the femoral artery prior to the acute drug injections was 3770 ± 860 (dynes sec cm^{-5}). Figure 4.2 shows the separated forward and backward waves after acute vasoactive drug injection in the same rat. There is an increased backward wave after treatment with norepinephrine and a decreased backward wave after treatment with sodium nitroprusside. From these representative waves, it was then possible to calculate characteristic impedance, reflection index, and magnitude of forward and backward waves. More importantly, it is evident that we were successful in separating forward and backward waves with a noticeable difference in amplitude of the backward wave after injection of vasoactive drugs. However, quantitative assessment of all data from all rats needed to be examined next to determine whether these measures were sufficiently sensitive to detect the changes.

Table 4.1 shows the effect of a saline vehicle, norepinephrine, and sodium nitroprusside on reflection index, characteristic impedance, CA PSV, and heart rate. The wave separation analysis parameters reflection index and characteristic impedance did not vary significantly with vasoactive drug injection, indicating that with a sample size of ten rats, they are not reliable indicators of arterial stiffness. However, reflection index responded as expected, increasing when the artery is stiffened with norepinephrine injection and decreasing when the artery is dilated with sodium nitroprusside injection. Characteristic impedance did not respond as expected to acute vasoactive drug injections characteristic impedance decreased in response to both norepinephrine and sodium nitroprusside injection. The clinically important measure of arterial stiffness CA PSV showed a trend to decrease with norepinephrine injection and increase with sodium nitroprusside injection, but it was not significantly different from saline control. CA PSV should increase as artery is constricted with norepinephrine and decrease as the artery is widened with sodium nitroprusside [99]. This is the opposite of what was found, possibly because of the mechanisms through which the carotid artery acutely regulates blood flow to the brain or due to the low sample size of four rats during the pulsed waveform ultrasound procedure. CA PSV is not a reliable indicator of arterial stiffness with acute vasoactive drug administration and low sample size in this experiment. Heart

rate varied only slightly with treatment and was not significant and therefore, heart rate's confounding effect on interpretation of CA PSV, systolic blood pressure, diastolic blood pressure, and pulse pressure can be ignored.

Figure 4.3 shows the significant effects of a saline vehicle, norepinephrine, and sodium nitroprusside on traditional blood pressure measures systolic blood pressure, diastolic blood pressure, and pulse pressure, and the WSA parameter amplitude of the backward wave. As expected, norepinephrine injection caused a significant increase in traditional blood pressure parameters systolic blood pressure, diastolic blood pressure, and pulse pressure. The increase in these parameters can be attributed to an increase in arterial stiffness after norepinephrine administration. Additionally, sodium nitroprusside caused a significant decrease in traditional blood pressure parameters systolic blood pressure, diastolic blood pressure, and pulse pressure. The decrease in these parameters could be attributed to a decrease in arterial stiffness and vasodilation of the capillary beds as seen by the decreased backward wave seen qualitatively in Figure 4.2. The wave separation analysis parameter, amplitude of the backward wave, increased significantly with norepinephrine stiffening of the artery and remained relatively unchanged with sodium nitroprusside injection. This indicates that the amplitude of the backward wave can detect arterial stiffening due to norepinephrine at a sample size of ten rats. With sodium nitroprusside injection, the vasodilation secondary to isoflurane anesthesia may be interfering with the effect of sodium nitroprusside at the femoral artery [59]. The amplitude of the backward wave was the most sensitive at detecting change from wave separation analysis parameters measured at the femoral artery in rats.

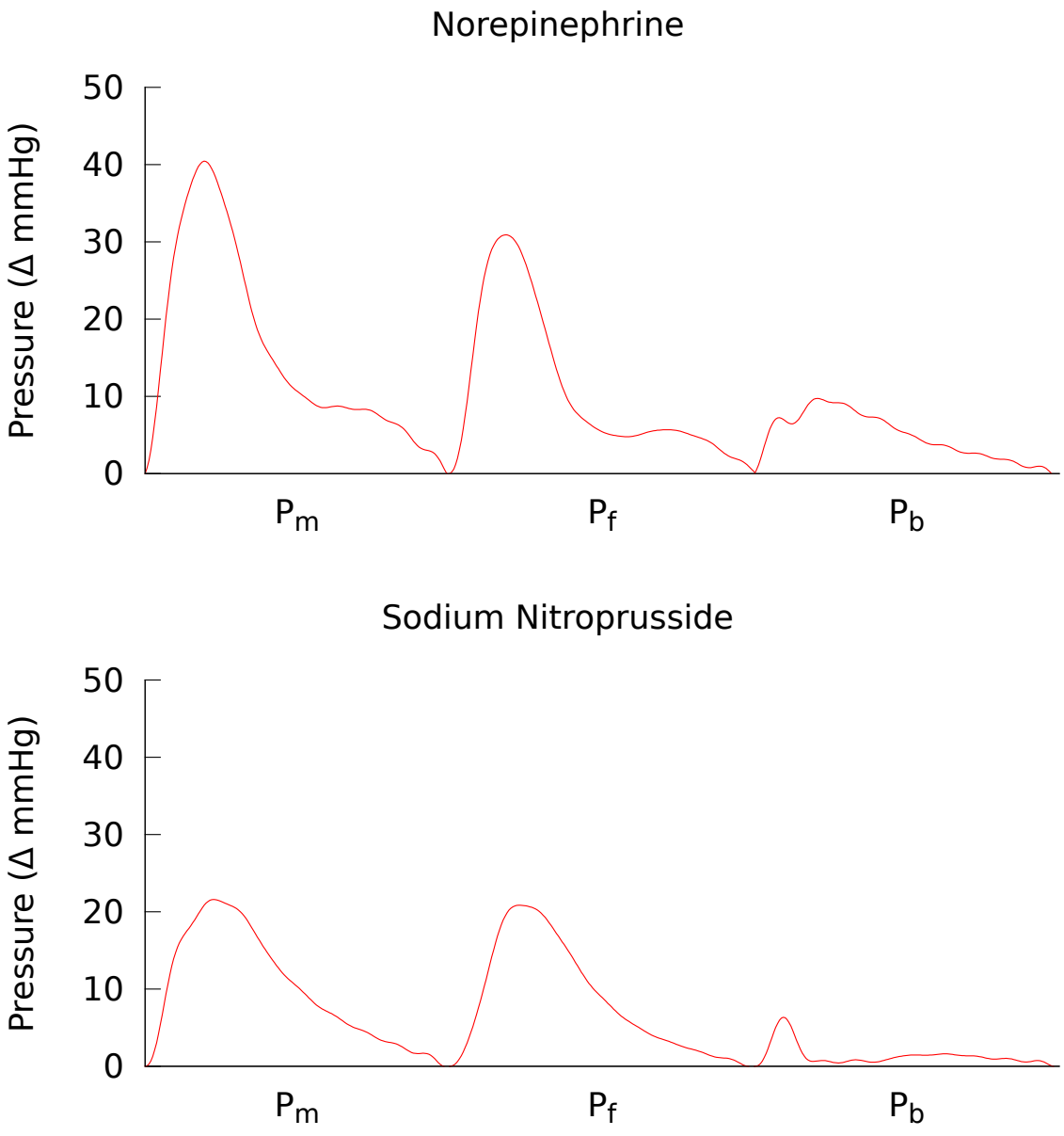

Figure 4.2: Pressure pulse waveform measured in the left femoral artery after intravenous injection of norepinephrine (0.02 mg/kg; top), and sodium nitroprusside (0.05 mg/kg; bottom) in the same rat. P_m is the measured pressure wave, P_f is the forward pressure wave, and P_b is the backward pressure wave. The shape of the pulse waveform and the size of the backward pressure wave changes with differing degrees of stiffness.

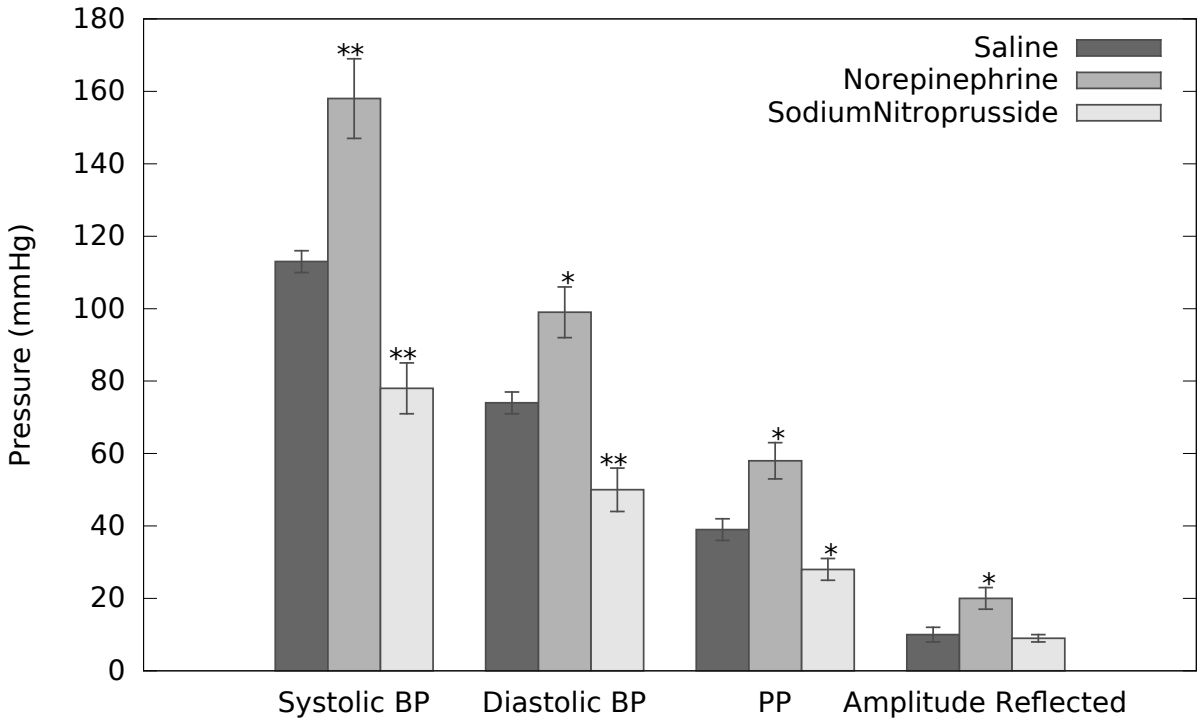

Figure 4.3: Effect of vasoactive drugs norepinephrine (0.02 mg/kg) and sodium nitroprusside (0.05 mg/kg) versus saline vehicle on systolic blood pressure, diastolic blood pressure, pulse pressure, and amplitude of the backward wave, in 10 healthy anesthetized rats. Note: *, $p < 0.05$ versus control (Saline) treatment in Dunnett's a posteriori test after one-way ANOVA with repeated measures.

Table 4.1: Effect of vasoactive drugs norepinephrine (0.02 mg/kg) and sodium nitroprusside (0.05 mg/kg) versus saline vehicle on reflection index, characteristic impedance, CA PSV, and heart rate. Values expressed as mean and standard error. Note: *, $p < 0.05$ versus control (Saline) group in Dunnett's a posteriori test after one-way ANOVA with repeated measures.

	Treatment		
	Saline	Norepinephrine	Sodium Nitroprusside
Reflection Index (%) n=10	25 ± 3	30 ± 3	23 ± 2
Characteristic Impedance (Z_c) (dynes sec cm^{-5}) n=10	3481 ± 761	2573 ± 401	2580 ± 1280
CA PSV ($\frac{\texttt{mm}}{\texttt{sec}}$) n=4	592 ± 182	337 ± 64	702 ± 143
TT (millisec) n=4	20 ± 1	16 ± 2*	15 ± 1*
Heart Rate ($\frac{\texttt{beats}}{\texttt{min}}$) n=10	374 ± 9	358 ± 12	374 ± 11

4.5 Discussion

The primary discovery of this study was that wave reflections are present and can be mathematically separated for quantification in the femoral artery in rats after acute vasoactive drug injections. A backward wave could be manipulated by vasoactive drug administration that was seen qualitatively on the pressure pulse waveform and measured quantitatively by wave separation analysis. The novel peripheral artery wave separation analysis technique and `WSanalyze` software provide a valuable and sensitive indicator of measuring arterial stiffness, by means of the amplitude of the backward wave in the femoral artery.

Traditionally, systolic blood pressure and pulse pressure measured through the brachial artery cuff oscillimetry is used as a cardiovascular indicator for arterial stiffness and a predictor of cardiovascular mortality [108]. Brachial artery cuff oscillimetry blood pressure overestimates cardiovascular disease because amplification of the pressure pulse occurs in the periphery [108]. Brachial artery cuff oscillimetry blood pressure has fallen out of favor for early prediction of cardiovascular mortality and several consensus statements have declared pulse wave velocity and wave separation analysis more effective at predicting cardiovascular

mortality in humans [127]. The major issue for preclinical and mechanistic biomedical researchers is that there are not currently equivalent tools readily available to measure these same parameters in rodent models for human disease, with wave separation analysis being the most notable lack. Thus, the importance of developing and validating tools for biomedical researchers to measure similar variables in rodents is of vital importance.

In this study, diastolic blood pressure increased with norepinephrine injection due to increase in vasoconstriction in the periphery from stimulation of the arteriole α_1 receptors. Systolic blood pressure increased with norepinephrine injection as expected from increased peripheral resistance and augmentation of the pressure pulse from earlier return of the backward pressure wave [87]. Diastolic blood pressure decreased with sodium nitroprusside injection due to vasodilation of the arterioles. Sodium nitroprusside breaks down into nitric oxide within the circulatory system [31]. Nitric oxide induces vasodilation of the arterioles by the arterial smooth muscle through activation of guanylyl cyclase and increased cGMP production [31]. Systolic blood pressure decreased with sodium nitroprusside injection due to a decrease in peripheral resistance and later arrival of the backward pressure wave. The observed blood pressure changes were as expected for the vasoactive drug experiment protocol. However, these blood pressure measurements do not reliably indicate arterial stiffness [127]. For that reason, clinicians have relied on other measures of arterial stiffness such as CA PSV or pulse wave velocity.

We found that CA PSV did not increase with norepinephrine injections as expected and did not decrease with sodium nitroprusside injections as expected. The opposite effect of vasoactive injections cannot be explained by the confounding effect of pressure dependency of CA PSV [111]. With the increase in pulse pressure seen with injection of a vasoconstrictor, norepinephrine, we expect a higher CA PSV and with the decrease in pulse pressure seen with injection of a vasodilator, sodium nitroprusside, we expect a lower CA PSV [111]. Pulse wave velocity was evaluated indirectly through TT at the carotid artery, TT decreased with norepinephrine as expected. However, TT also decreased with sodium nitroprusside which is the opposite of what was predicted. This suggests that the rat carotid artery does not behave as expected when vasoactive drugs are administered as an intravenous bolus. Additionally, the segment of data chosen for analysis 30 seconds after the injection of vasoactive drugs may

not represent the greatest treatment effect. This time frame for sampling was chosen based on blood pressure changes in preliminary experiments but may not represent maximal arterial stiffening. This study highlights that traditional measures of arterial stiffness, particularly CA PSV and TT, a similar measurement to pulse wave velocity, are susceptible to other effects that impair the ability to detect changes in arterial stiffness [72]. New robust measures of arterial stiffness are needed for rodent cardiovascular research.

This study also provides reference ranges for characteristic impedance measured at the carotid and femoral artery in rats, important values for biophysical studies such as this that had not been previously determined in rats to our knowledge. The method of measuring characteristic impedance in the femoral and carotid artery damages the endothelium through catheter insertion [110]. Arterial stiffness will increase with damaged endothelium theoretically increasing characteristic impedance [110]. An ex vivo theoretical measurement of characteristic impedance in a section of rat carotid artery was of the same magnitude but larger than the values measured in this study [25]. An in vivo measurement of characteristic impedance in the rat aorta, 5200 $\pm$ 1200 dynes sec cm^{-5}, was of the same magnitude as the characteristic impedance measured at the carotid and femoral artery in this study [80]. The similarity in characteristic impedance at the carotid and femoral artery to values previously reported in the rat aorta increases the confidence in the method used to collect data and the `WSanalyze` software. Aortic characteristic impedance has been used to explore the effects on the rat vasculature of nitric oxide, aging, left ventricular hypertrophy, hypertension, calcification of arteries, chronic renal failure, and diabetes [44, 18, 20, 67, 24, 105]. Femoral characteristic impedance did not vary enough to be used as a measure of arterial stiffness in this acute vasoactive drug experiment. However, measuring wave reflection in this acute vasoactive drug experiment was an indicator of arterial stiffness.

Wave reflection was assessed by reflection index and amplitude of the backward pressure wave. Reflection index showed the expected trend of increasing with norepinephrine injection and decreasing with sodium nitroprusside injection, but it was not a sensitive enough indicator of arterial stiffness to be used alone. Reflection index is calculated using the forward and backward pressure wave and the variation the forward pressure wave from the effect of volume bolus drug administration on the heart may be a confounder in this experiment.

The amplitude of the backward wave amplitude has been shown to be the most consistent long-term wave separation analysis predictor independent of blood pressure of cardiovascular morbidity and mortality in humans [131]. Furthermore, the backward wave amplitude has been shown to predict cardiovascular morbidity and mortality equally well in men and women independent of pulse wave velocity; whereas reflection index has been only shown to predict cardiovascular morbidity and mortality in men [128]. This study confirmed results found in human clinical trials for preclinical rodent biomedical research; the amplitude of the backward wave is the most sensitive wave separation analysis parameter measured by `WSanalyze` for detecting arterial stiffness.

Norepinephrine injection caused an increase in the amplitude of the backward pressure wave as expected from α_1-mediated vasconstriction. There was no difference in the backward pressure waves between sodium nitroprusside and saline injection. Because sodium nitroprusside is a nitric oxide donor, the vasodilatory effect it has may be masked by the vasodilation caused by isoflurane [59]. Thus, the inability to detect a significant change in backward wave amplitude after sodium nitroprusside injection in anesthetized rats is not taken as an indication of limitation of this parameter, but rather it is interpreted as detecting the underlying lack of change in this parameter in a situation of vasodilation.

This study provides a new method measuring arterial stiffness in rats that is validated for use with acute arterial stiffness changes induced by vasoactive drugs. Wave separation analysis in the femoral artery with `WSanalyze` can help researchers in determining the vascular effect and mechanism of vasoactive drugs and may be equally successful if used in a chronic model of cardiovascular disease that leads to arterial stiffness. The femoral artery measurement of wave reflections validated in this study is technically easier than aortic measurement of wave reflections. This technique provides a sensitive measure of arterial stiffness, backward wave amplitude, for preclinical and mechanistic researchers that use rodents as models for human disease.

Chapter 5

Future Work and Conclusions

This thesis contributes to the development of new techniques of indicating and measuring arterial stiffness in the rat. Two methods of measuring arterial stiffness were developed for use in the femoral artery: pulse waveform analysis parameter dP/dt_{min} and wave separation analysis. From the wave separation analysis parameters, the amplitude of the backward wave is the most promising measure of arterial stiffness. The methods were developed by outlining the surgical approaches to employ these new methods, describing the mathematical and physical processing of calculating these new methods, and software development required to analyze and report the measures of arterial stiffness from experimental data. Arterial stiffness was induced in rats in chronic studies with varying levels of vitamin D. Additionally, arterial stiffness was induced in rats in acute studies with vasoactive drug injections with acetylcholine, norepinephrine, and sodium nitroprusside. The validity of the arterial stiffness indices dP/dt_{min}, dP/dt_{max}, and backward wave amplitude, Z_c, and RI were then compared in these rat models of arterial stiffness. The most sensitive arterial stiffness indicies are dP/dt_{min}, dP/dt_{max}, and backward wave amplitude for changes in arterial stiffness.

5.1 Summary of Results

5.1.1 Using dP/dt_{min} to Measure Arterial Stiffness in Rats

Pulse waveform analysis parameters were investigated using the rat femoral artery in Chapter 2 of this thesis. Implantation of blood pressure telemetry devices in the femoral artery provided continuous blood pressure monitoring capability for chronic hemodynamic experiments. The femoral artery blood pressure trace shape can be analyzed into a set of cardiovascular

parameters: systolic blood pressure, diastolic blood pressure, pulse pressure, dP/dt_{min}, and dP/dt_{max}. The software `PWanalyze` was developed to calculate this set of parameters from the measured blood pressure data. `PWanalyze` has a graphical user interface that is used to input data files, select relevant areas of the blood pressure trace to be analyzed, and export the results in both textual and graphical formats. In the current study, varying levels of vitamin D supplementation were fed chronically to rats. The range of arterial stiffness produced was used to show that dP/dt_{min} was an equally good indicator of arterial stiffness in comparison to dP/dt_{max}. A follow-up study with acute vasoactive drug injection showed that the changes in dP/dt_{min} and dP/dt_{max} were consistent with an increase in arterial stiffness caused by norepinephrine injection and a decrease in arterial stiffness caused by acetylcholine injection. The performance of dP/dt_{min} was similar to dP/dt_{max}, but it may be slightly better at detecting changes in chronic arterial stiffness because it varied significantly with varying levels of vitamin D supplementation, whereas dP/dt_{max} did not. Biomedical researchers should add dP/dt_{min} and dP/dt_{max} to their study any time intra-arterial blood pressure is taken to gain valuable insight into arterial stiffness.

5.1.2 Using Wave Separation Analysis to Measure Arterial Stiffness in Rats

Wave separation analysis was adapted to assess wave reflection in the rat peripheral arteries in Chapter 4. The left and right carotid and femoral arteries were selected to develop a peripheral artery wave separation analysis technique in the rat. A new adaptation of the original wave separation analysis method to peripheral arteries was outlined. The indices calculated by wave separation analysis include backward wave amplitude, Z_c, and RI. The custom software `WSanalyze`, was developed to calculate the wave separation analysis indices. `WSanalyze` allows the user to specify an experimental data file and select relevant areas of the blood pressure trace to analyze. Wave separation analysis indices are then are output in graph and text form. An acute drug injection experiment using norepinephrine and sodium nitroprusside demonstrated that backward waves could be observed in the femoral artery using this new wave separation analysis adaptation. Backward waves could be seen to increase

both qualitatively and quantitatively in the femoral artery with injection of norepinephrine. The results from the new wave separation analysis adaptation agreed with the original wave separation analysis method because the characteristic impedance calculated with the new method was found to be of the same magnitude as aortic characteristic impedance and ex vivo carotid artery characteristic impedance reported previously [25, 80]. Backward wave amplitude is recommended for measuring arterial stiffness in the femoral artery of rats.

5.1.3 dP/dt_{min} Versus Backward Wave Amplitude

The measurement of dP/dt_{min} is recommended for every pre-clinical cardiovascular study in rodents where the cardiovascular effects of disease, pharmaceuticals, or toxins are being investigated through effects on blood pressure. The use of dP/dt_{min} has been validated with intra-arterial blood pressure measurement in this study at the femoral and iliac artery. Backward wave amplitude is the most sensitive indicator of arterial stiffness found in this thesis. The use of backward wave amplitude has been validated at the femoral artery in rats with paired measurement of flow at the right femoral artery and pressure at the left femoral artery simultaneously.

Both dP/dt_{min} and backward wave amplitude have not been validated at locations other than the femoral artery at this time. Measurement of dP/dt_{min} is easier than backward wave amplitude because it only involves blood pressure measurement. This will enable researchers to use blood pressure telemetry and measure dP/dt_{min} in conscious unrestrained animals, whereas backward wave amplitude is measured in a terminal procedure under anesthesia at this time. However, backward wave amplitude has been shown to be increasingly more accurate in humans for predicting cardiovascular morbidity and mortality, and therefore, its addition to pre-clinical rodent cardiovascular studies is invaluable. Backward wave amplitude should be used by researchers to measure arterial stiffness in rats undergoing terminal procedures and dP/dt_{min} should be used when measurement of backward wave amplitude is impractical.

5.2 Future Work

This section outlines future work that needs to be performed to strengthen the case for femoral artery pulse waveform analysis and wave separation analysis to become accepted measures of arterial stiffness in comparative biomedical studies.

5.2.1 Continuous rate infusion experiment

In Chapters 2 and 4, injection of vasoactive drugs was used to create acute changes in arterial stiffness. The addition of the volume of the injection, called the volume bolus, has a confounding effect on the experiment. The volume bolus increases the central venous pressure which triggers the bainbridge reflex. The bainbridge reflex increases heart rate in response to the increase of blood volume in the central veins. To filter out the volume bolus effect in the current experiments, saline was injected in the same volume as the vasoactive drugs. The saline injection was used to control for the volume bolus effect. However, the volume bolus effect could be completely eliminated in future experiments if the vasoactive drugs were given by continuous rate infusions. The vascular effects of bolus drug administration versus a continuous rate infusion could then be characterized for pulse waveform analysis and wave separation analysis in the rat peripheral arteries. Additionally, a continuous rate infusion of vasoactive drugs would avoid the potential problem that the segment of data chosen for analysis after the injection of vasoactive drugs may not represent the greatest treatment effect. A continuous rate infusion experiment would establish how pulse waveform analysis and wave separation analysis parameters vary with the bainbridge reflex and help future researchers interpret pulse waveform analysis and wave separation analysis parameters when a volume bolus is part of the experiment.

5.2.2 Characterization of pressure and heart rate dependency

Pressure and heart rate affect pulse wave velocity measurements. The effect of pressure and heart rate on wave separation analysis parameters in the rat is not known, but it has been assumed to be less than effects on pulse pressure or dP/dt_{max} [26, 33]. However, this

assumption is untested. To investigate this further, a chronic arterial stiffening treatment could be administered to the rats and then the blood pressure and heart rate could be altered pharmacologically. The wave separation analysis parameters would then be compared between the treated rats and the control rats at a variety of pressures and heart rates. This would establish whether wave separation analysis must be compared at the same pressures and heart rates to meaningfully compare arterial stiffness between different treatments and offer further validation to these novel measures of arterial stiffness.

5.2.3 Comparison to central arterial dynamics

This thesis involves using wave separation analysis techniques in the femoral artery of the rat. Wave separation analysis has been used by previous researchers in the aorta but not the femoral artery. In order for wave separation analysis to be adopted in the femoral artery as a standard technique, it must be shown that arterial stiffness measurements do not vary between sites. To confirm that the femoral artery may be used to measure arterial stiffness, backward waves should be compared between the ascending aorta and femoral artery in the same rats under the same pathophysiological or pharmacological states. The ideal comparison would be with a rat that does not need to be mechanically ventilated from a thoracotomy during data collection. To achieve this, the blood pressure in the ascending aorta could be measured by a blood pressure telemetry device introduced through the carotid artery. The blood flow of the ascending aorta could be obtained by a chronic thoracotomy technique where after placement of the flow probe, negative pleural pressure is re-established in the thorax and the rat is recovered. Both surgical approaches for blood pressure and flow measurement are possible and have been documented previously in rats. From this experiment, we would be able to see the predictive power of wave separation analysis techniques in the femoral artery of estimating the central arterial hemodynamics and general cardiovascular morbidity and mortality.

5.2.4 Comparison to the carotid artery

The femoral artery was used in this thesis to measure arterial stiffness with pulse waveform analysis and wave separation analysis. The carotid artery might also be a suitable candidate for peripheral artery measurement of arterial stiffness. Further work is needed to characterize how pulse waveform analysis and wave separation analysis indices in the carotid artery vary from the femoral artery. The carotid artery is involved in regulating blood flow to the brain, which has controls that are often separate from the rest of the systemic circulation and may be a confounding factor to the measurement of arterial stiffness in low blood pressure states. Future work involves comparing the carotid artery to the femoral artery in rats in hypotension, normotension, and hypertension. Currently, the femoral artery is the most promising site for pulse waveform analysis and wave separation analysis; however, the carotid artery may be a suitable alternative if the effects of blood pressure in the carotid artery are fully investigated for pulse waveform analysis and wave separation analysis parameters.

5.2.5 Chronic arterial stiffening measurement

The goal of this study is to provide techniques that can be used in chronic arterial stiffening studies. The natural extension of this research is to apply the methods of pulse waveform analysis and wave separation analysis to rat models of atherosclerosis and chronic cardiovascular disease. In order for pulse waveform analysis and wave separation analysis to be adapted as valuable tools by the biomedical research community, their utility in exploring the effects of common diseases (i.e., high cholesterol, hypertension, and diabetes) on the arterial system must be demonstrated.

5.3 Conclusion

All of the hypotheses in Section 1.7 were shown to be true. The theory behind wave separation analysis was outlined and a peripheral artery technique for wave separation analysis was developed. Open source software was developed to calculate dP/dt_{min}. Software was also developed to calculate wave separation analysis and is available upon request. Acute

and chronic experiments showed that dP/dt_{min} and backward wave amplitude are superior measures of arterial stiffness.

With the results of the current thesis and further strengthening from the proposed future experiments, pulse waveform analysis and wave separation analysis could become reliable, important tools for preclinical cardiovascular researchers. By writing software and providing free access to all researchers, the hope is to facilitate the uptake of this technology, improve the quality of information provided in cardiovascular studies, and ultimately improve health of all species, including humans.

References

[1] Ibhar Al Mheid, Riyaz Patel, Jonathan Murrow, Alanna Morris, Ayaz Rahman, Lucy Fike, Nino Kavtaradze, Irina Uphoff, Craig Hooper, Vin Tangpricha, R Wayne Alexander, Kenneth Brigham, and Arshed A Quyyumi. Vitamin D status is associated with arterial stiffness and vascular dysfunction in healthy humans. *Journal of the American College of Cardiology*, 58(2):186–92, jul 2011.

[2] Peter Alagona and Tariq Ali Ahmad. Cardiovascular disease risk assessment and prevention: current guidelines and limitations. *The Medical clinics of North America*, 99(4):711–31, jul 2015.

[3] Kerstin Amann. Media calcification and intima calcification are distinct entities in chronic kidney disease. *Clinical journal of the American Society of Nephrology : CJASN*, 3(6):1599–605, nov 2008.

[4] Grethe Neumann Andersen, Lucia Mincheva-Nilsson, Elsadig Kazzam, Gunnar Nyberg, Natalia Klintland, Ann-Sofi Petersson, Solbritt Rantapää-Dahlqvist, Anders Waldenström, and Kenneth Caidahl. Assessment of vascular function in systemic sclerosis: indications of the development of nitrate tolerance as a result of enhanced endothelial nitric oxide production. *Arthritis and rheumatism*, 46(5):1324–32, may 2002.

[5] David Ascher and Paul F Dubois. Numerical Python. *Computers in Physics*, 10:262–267, 2001.

[6] Atcor Medical. Technical Note 9 Validation and Reproducibility of SphygmoCor Px.

[7] Jeffrey Atkinson. Age-related medial elastocalcinosis in arteries: mechanisms, animal models, and physiological consequences. *Journal of applied physiology (Bethesda, Md. : 1985)*, 105(5):1643–51, nov 2008.

[8] Alberto Avolio. Input impedance of distributed arterial structures as used in investigations of underlying concepts in arterial haemodynamics. *Medical & biological engineering & computing*, 47(2):143–51, feb 2009.

[9] Alexandre Benjo, Richard E Thompson, Derek Fine, Charles W Hogue, Diane Alejo, Anita Kaw, Gary Gerstenblith, Ashish Shah, Dan E Berkowitz, and Daniel Nyhan. Pulse pressure is an age-independent predictor of stroke development after cardiac surgery. *Hypertension*, 50(4):630–5, oct 2007.

[10] J. Blacher, B. Pannier, A. P. Guerin, S. J. Marchais, M. E. Safar, and G. M. London. Carotid Arterial Stiffness as a Predictor of Cardiovascular and All-Cause Mortality in End-Stage Renal Disease. *Hypertension*, 32(3):570–574, sep 1998.

[11] J M Bland and D G Altman. Measuring agreement in method comparison studies. *Statistical methods in medical research*, 8(2):135–60, jun 1999.

[12] Mari E Boesen, Dilip Singh, Bijoy K Menon, and Richard Frayne. A systematic literature review of the effect of carotid atherosclerosis on local vessel stiffness and elasticity. *Atherosclerosis*, 243(1):211–22, nov 2015.

[13] Barry A Borlaug and David A Kass. Invasive hemodynamic assessment in heart failure. *Heart failure clinics*, 5(2):217–28, apr 2009.

[14] Mark Butlin, George Lindesay, Kayla D Viegas, and Alberto P Avolio. Pressure dependency of aortic pulse wave velocity in vivo is not affected by vasoactive substances that alter aortic wall tension ex vivo. *American journal of physiology. Heart and circulatory physiology*, 308(10):H1221–8, may 2015.

[15] Marina Cecelja, Benyu Jiang, Karen McNeill, Bernet Kato, James Ritter, Tim Spector, and Phil Chowienczyk. Increased wave reflection rather than central arterial stiffness is the main determinant of raised pulse pressure in women and relates to mismatch in arterial dimensions: a twin study. *Journal of the American College of Cardiology*, 54(8):695–703, aug 2009.

[16] K.-C. Chang, C.-D. Tseng, T.-F. Chou, Y.-L. Cho, T.-C. Chi, M.-J. Su, and Y.-Z. Tseng. Arterial stiffening and cardiac hypertrophy in a new rat model of type 2 diabetes. *European Journal of Clinical Investigation*, 36(1):1–7, jan 2006.

[17] Kuo-Chu Chang, Kwan-Lih Hsu, Chuen-Den Tseng, Yue-Der Lin, Yi-Li Cho, and Yung-Zu Tseng. Aminoguanidine prevents arterial stiffening and cardiac hypertrophy in streptozotocin-induced diabetes in rats. *British journal of pharmacology*, 147(8):944–50, apr 2006.

[18] Kuo-Chu Chang, Yuan-Feen Tsai, Chai-Yee Chow, Ying-I Peng, and Tong-J Chen. Age-related changes of arterial mechanical properties in rats: analysis using exponentially tapered T-tube model. *The journals of gerontology. Series A, Biological sciences and medical sciences*, 53(4):B274–80, jul 1998.

[19] H I Chen and C T Hu. Endogenous nitric oxide on arterial hemodynamics: a comparison between normotensive and hypertensive rats. *The American journal of physiology*, 273(4 Pt 2):H1816–23, oct 1997.

[20] H I Chen, C T Hu, and K C Chang. Characterization of arterial hemodynamics in rats with established hypertension. *The Chinese journal of physiology*, 39(1):49–55, jan 1996.

[21] Wei Chen, Shengxu Li, Camilo Fernandez, Dianjianyi Sun, Chin-Chih Lai, Tao Zhang, Lydia Bazzano, Elaine M Urbina, and Hong-Wen Deng. Temporal Relationship Between Elevated Blood Pressure and Arterial Stiffening Among Middle-Aged Black and White Adults: The Bogalusa Heart Study. *American journal of epidemiology*, 183(7):599–608, apr 2016.

[22] Tain-Junn Cheng, Jiunn-Jye Chuu, Chia-Yu Chang, Wan-Chen Tsai, Kuan-Jung Chen, and How-Ran Guo. Atherosclerosis induced by arsenic in drinking water in rats through altering lipid metabolism. *Toxicology and applied pharmacology*, 256(2):146–53, oct 2011.

[23] Yun-Seok Choi, Ho-Joong Youn, Jeong-Sook Youn, Chul-Soo Park, Yong-Seog Oh, and Wook-Sung Chung. Measurement of the intimal thickness of the carotid artery: comparison between 40 MHz ultrasound and histology in rats. *Ultrasound in medicine & biology*, 35(6):962–6, jun 2009.

[24] Yao-Chen Chuang, Ming-Shiou Wu, Yi-Kai Su, and Kwang-Ming Fang. Effects of olmesartan on arterial stiffness in rats with chronic renal failure. *Cardiovascular Diabetology*, 11(1):66, jan 2012.

[25] R H Cox. Comparison of carotid artery mechanics in the rat, rabbit, and dog. *The American journal of physiology*, 234(3):H280–8, mar 1978.

[26] Anthony M Dart and Bronwyn A Kingwell. Pulse pressurea review of mechanisms and clinical relevance. *Journal of the American College of Cardiology*, 37(4):975–984, mar 2001.

[27] Claire de Oliveira, Van Hai Nguyen, Harindra C Wijeysundera, William W L Wong, Gloria Woo, Peter P Liu, and Murray D Krahn. How much are we spending? The estimation of research expenditures on cardiovascular disease in Canada. *BMC health services research*, 12:281, jan 2012.

[28] Julius L Decano, Jason C Viereck, Ann C McKee, James A Hamilton, Nelson Ruiz-Opazo, and Victoria L M Herrera. Early-life sodium exposure unmasks susceptibility to stroke in hyperlipidemic, hypertensive heterozygous Tg25 rats transgenic for human cholesteryl ester transfer protein. *Circulation*, 119(11):1501–9, mar 2009.

[29] D E Dick, J E Kendrick, G L Matson, and V C Rideout. Measurement of nonlinearity in the arterial system of the dog by a new method. *Circulation research*, 22(2):101–11, feb 1968.

[30] Stanley S Franklin, Sohum S Gokhale, Vincent H Chow, Martin G Larson, Daniel Levy, Ramachandran S Vasan, Gary F Mitchell, and Nathan D Wong. Does low diastolic blood pressure contribute to the risk of recurrent hypertensive cardiovascular disease events? The Framingham Heart Study. *Hypertension*, 65(2):299–305, feb 2015.

[31] J A Friederich and J F Butterworth. Sodium nitroprusside: twenty years and counting. *Anesthesia and analgesia*, 81(1):152–62, jul 1995.

[32] Balázs Gaszner, Zsófia Lenkey, Miklós Illyés, Zsolt Sárszegi, Iván G Horváth, Balázs Magyari, Ferenc Molnár, Attila Kónyi, and Attila Cziráki. Comparison of aortic and carotid arterial stiffness parameters in patients with verified coronary artery disease. *Clinical cardiology*, 35(1):26–31, jan 2012.

[33] Nicole J Gentner and Lynn P Weber. Using blood pressure telemetry to assess acute changes in arterial stiffness in rats after nitric oxide synthase inhibition or environmental tobacco smoke exposure. *Canadian journal of physiology and pharmacology*, 88(9):918–28, sep 2010.

[34] Nicole J Gentner and Lynn P Weber. Intranasal benzo[a]pyrene alters circadian blood pressure patterns and causes lung inflammation in rats. *Archives of toxicology*, 85(4):337–46, apr 2011.

[35] Nicole J Gentner and Lynn P Weber. Secondhand tobacco smoke, arterial stiffness, and altered circadian blood pressure patterns are associated with lung inflammation and oxidative stress in rats. *American journal of physiology. Heart and circulatory physiology*, 302(3):H818–25, feb 2012.

[36] Edward G Grant, Carol B Benson, Gregory L Moneta, Andrei V Alexandrov, J Dennis Baker, Edward I Bluth, Barbara A Carroll, Michael Eliasziw, John Gocke, Barbara S Hertzberg, Sandra Katarick, Laurence Needleman, John Pellerito, Joseph F Polak, Kenneth S Rholl, Douglas L Wooster, and Eugene Zierler. Carotid artery stenosis: grayscale and Doppler ultrasound diagnosis–Society of Radiologists in Ultrasound consensus conference. *Ultrasound quarterly*, 19(4):190–8, dec 2003.

[37] Heynric B Grotenhuis, Jos J M Westenberg, Paul Steendijk, Rob J van der Geest, Jaap Ottenkamp, Jeroen J Bax, J Wouter Jukema, and Albert de Roos. Validation and reproducibility of aortic pulse wave velocity as assessed with velocity-encoded MRI. *Journal of magnetic resonance imaging : JMRI*, 30(3):521–6, sep 2009.

[38] Alvaro N Gurovich, Darren T Beck, and Randy W Braith. Aortic Pulse Wave Analysis is not a surrogate for central arterial Pulse Wave Velocity. *Experimental biology and medicine (Maywood, N.J.)*, 234(11):1339–44, nov 2009.

[39] Evelien Hermeling, Arnold P G Hoeks, Mark H M Winkens, Johannes L Waltenberger, Robert S Reneman, Abraham A Kroon, and Koen D Reesink. Noninvasive assessment of arterial stiffness should discriminate between systolic and diastolic pressure ranges. *Hypertension*, 55(1):124–30, jan 2010.

[40] Evelien Hermeling, Koen D Reesink, Arnold P G Hoeks, and Robert S Reneman. Modeled decomposition of aortic pressure waveforms does not provide estimates for pulse wave velocity. *Hypertension*, 51(6):e60; author reply e61, jun 2008.

[41] Victoria L Herrera, Julius L Decano, Nicholas Giordano, Ann Marie Moran, and Nelson Ruiz-Opazo. Aortic and carotid arterial stiffness and epigenetic regulator gene expression changes precede blood pressure rise in stroke-prone Dahl salt-sensitive hypertensive rats. *PloS one*, 9(9):e107888, jan 2014.

[42] H Higashino, K Simeonova, I Lambev, M Markov, and A Suzuki. Proper measurement of blood pressure and heart rate in SHRSP and WKY by an indirect volume-oscillometric method. *Clinical and experimental pharmacology & physiology. Supplement*, 22(1):S292–3, dec 1995.

[43] C T Hu, K C Chang, C Y Wu, and H I Chen. Acute effects of nitric oxide blockade with L-NAME on arterial haemodynamics in the rat. *British journal of pharmacology*, 122(6):1237–43, nov 1997.

[44] Cheng-Tao Hu, Huai-Ren Chang, Yung-Hsiang Hsu, Chia-Jui Liu, and Hsing I Chen. Ventricular hypertrophy and arterial hemodynamics following deprivation of nitric oxide in rats. *Life sciences*, 78(2):164–73, nov 2005.

[45] Yanwu Hu, Bo Sun, Kai Liu, Mengtong Yan, Yang Zhang, Chunsheng Miao, and Liqun Ren. Icariin Attenuates High-cholesterol Diet Induced Atherosclerosis in Rats by Inhibition of Inflammatory Response and p38 MAPK Signaling Pathway. *Inflammation*, aug 2015.

[46] Daniel A Huetteman and Heather Bogie. Direct blood pressure monitoring in laboratory rodents via implantable radio telemetry. *Methods in molecular biology (Clifton, N.J.)*, 573:57–73, jan 2009.

[47] John Hunter and Michael Droettboom. matplotlib. In *The Architecture of Open Source Applications*, volume 2, pages 1–14. 2014.

[48] Jamila Ibrahim, Bradford C Berk, and Alun D Hughes. Comparison of simultaneous measurements of blood pressure by tail-cuff and carotid arterial methods in conscious spontaneously hypertensive and Wistar-Kyoto rats. *Clinical and experimental hypertension (New York, N.Y. : 1993)*, 28(1):57–72, jan 2006.

[49] David R Jacobs, Daniel A Duprez, and Daichi Shimbo. Invited Commentary: Hypertension and Arterial Stiffness-Origins Remain a Dilemma. *American journal of epidemiology*, 183(7):609–12, apr 2016.

[50] Gerard N. Jager, Nico Westerhof, and Abraham Noordergraaf. Oscillatory Flow Impedance in Electrical Analog of Arterial System:: Representation of Sleeve Effect and Non-Newtonian Properties of Blood. *Circulation Research*, 16(2):121–133, feb 1965.

[51] David Jegger, Rafaela da Silva, Xavier Jeanrenaud, Mohammad Nasratullah, Hendrik Tevaearai, Ludwig K von Segesser, Patrick Segers, Virginie Gaillard, Jeffrey Atkinson, Isabelle Lartaud, and Nikolaos Stergiopulo. Ventricular-arterial coupling in a rat model of reduced arterial compliance provoked by hypervitaminosis D and nicotine. *American journal of physiology. Heart and circulatory physiology*, 291(4):H1942–51, oct 2006.

[52] Hadassa M Jochemsen, Majon Muller, Michiel L Bots, Philip Scheltens, Koen L Vincken, Willem P T M Mali, Yolanda van der Graaf, and Mirjam I Geerlings. Arterial stiffness and progression of structural brain changes: The SMART-MR study. *Neurology*, 84(5):448–55, feb 2015.

[53] Bernhard M Kaess, Jian Rong, Martin G Larson, Naomi M Hamburg, Joseph A Vita, Daniel Levy, Emelia J Benjamin, Ramachandran S Vasan, and Gary F Mitchell. Aortic stiffness, blood pressure progression, and incident hypertension. *JAMA : the journal of the American Medical Association*, 308(9):875–81, sep 2012.

[54] Shin-ichiro Katsuda, Masamitsu Hasegawa, Masahiko Kusanagi, and Tsuyoshi Shimizu. Comparison of pulse-wave velocity in different aortic regions in relation to the extent and severity of atherosclerosis between young and older Kurosawa and Kusanagi-hypercholesterolemic (KHC) rabbits. *Clinical science (London, England : 1979)*, 99(5):393–404, nov 2000.

[55] Pascal Kieffer, Alain Robert, Christine Capdeville-Atkinson, Jeffrey Atkinson, and Isabelle Lartaud-Idjouadiene. Age-related arterial calcification in rats. *Life sciences*, 66(24):2371–81, may 2000.

[56] Mark J Kilgard. The opengl utility toolkit (glut) programming interface. 1996.

[57] Chang-Sei Kim, Nima Fazeli, M Sean McMurtry, Barry A Finegan, and Jin-Oh Hahn. Quantification of wave reflection using peripheral blood pressure waveforms. *IEEE journal of biomedical and health informatics*, 19(1):309–16, jan 2015.

[58] John G Kingma and P E Roy. Ultrastructural study of hypervitaminosis D induced arterial calcification in Wistar rats. *Artery*, 16(1):51–61, jan 1988.

[59] P Kirstetter, F Lagneau, O Lucas, Y Krupa, and J Marty. Role of endothelium in the modulation of isoflurane-induced vasodilatation in rat thoracic aorta. *British Journal of Anaesthesia*, 79(1):84–87, 1997.

[60] S Kobayashi, M Yano, M Kohno, M Obayashi, Y Hisamatsu, T Ryoke, T Ohkusa, K Yamakawa, and M Matsuzaki. Influence of aortic impedance on the development of pressure-overload left ventricular hypertrophy in rats. *Circulation*, 94(12):3362–8, dec 1996.

[61] Satoru Kodama, Chika Horikawa, Kazuya Fujihara, Sakiko Yoshizawa, Yoko Yachi, Shiro Tanaka, Nobumasa Ohara, Satoshi Matsunaga, Takaho Yamada, Osamu Hanyu, and Hirohito Sone. Meta-analysis of the quantitative relation between pulse pressure and mean arterial pressure and cardiovascular risk in patients with diabetes mellitus. *The American journal of cardiology*, 113(6):1058–65, mar 2014.

[62] Ted R Kohler and Arkadiusz Jawien. Flow affects development of intimal hyperplasia after arterial injury in rats. *Arteriosclerosis, Thrombosis, and Vascular Biology*, 12(8):963–971, aug 1992.

[63] Klaas Kramer and René Remie. Measuring blood pressure in small laboratory animals. *Methods in molecular medicine*, 108:51–62, 2005.

[64] Eleanore S J Kröner, Hildo J Lamb, Hans-Marc J Siebelink, Suzanne C Cannegieter, Pieter J van den Boogaard, Ernst E van der Wall, Albert de Roos, and Jos J M

Westenberg. Pulse wave velocity and flow in the carotid artery versus the aortic arch: effects of aging. *Journal of magnetic resonance imaging : JMRI*, 40(2):287–93, aug 2014.

[65] Theodore W Kurtz, Karen A Griffin, Anil K Bidani, Robin L Davisson, and John E Hall. Recommendations for blood pressure measurement in humans and experimental animals. Part 2: blood pressure measurement in experimental animals. *Hypertension*, 45:299–310, 2005.

[66] Pierre Lantelme, Christine Mestre, Michel Lievre, Alain Gressard, and Hugues Milon. Heart rate: an important confounder of pulse wave velocity assessment. *Hypertension*, 39(6):1083–7, jun 2002.

[67] Isabelle Lartaud-Idjouadiene, Anne-Marie Lompre, Pascal Kieffer, Thérèse Colas, and Jeffrey Atkinson. Cardiac Consequences of Prolonged Exposure to an Isolated Increase in Aortic Stiffness. *Hypertension*, 34(1):63–69, jul 1999.

[68] Stéphane Laurent, Pierre Boutouyrie, Roland Asmar, Isabelle Gautier, Brigette Laloux, Louis Guize, Pierre Ducimetiere, and Athanase Benetos. Aortic Stiffness Is an Independent Predictor of All-Cause and Cardiovascular Mortality in Hypertensive Patients. *Hypertension*, 37(5):1236–1241, may 2001.

[69] Stéphane Laurent, John Cockcroft, Luc Van Bortel, Pierre Boutouyrie, Cristina Giannattasio, Daniel Hayoz, Bruno Pannier, Charalambos Vlachopoulos, Ian Wilkinson, and Harry Struijker-Boudier. Expert consensus document on arterial stiffness: methodological issues and clinical applications. *European heart journal*, 27(21):2588–605, nov 2006.

[70] Stéphane Laurent, John Cockcroft, Luc Van Bortel, Pierre Boutouyrie, Cristina Giannattasio, Daniel Hayoz, Bruno Pannier, Charalambos Vlachopoulos, Ian Wilkinson, and Harry Struijker-Boudier. Abridged version of the expert consensus document on arterial stiffness. *Artery Research*, 1(1):2–12, jun 2007.

[71] Chen-Chin Lee and Rodger G Mark. Analysis of arterial waves by the single-pulse-response method. *IEEE transactions on bio-medical engineering*, 40(8):833–6, aug 1993.

[72] Ching Wei Lee, Shih Hsien Sung, Chun Ku Chen, I Ming Chen, Hao Min Cheng, Wen Chung Yu, Chun Che Shih, and Chen Huan Chen. Measures of carotid-femoral pulse wave velocity and augmentation index are not reliable in patients with abdominal aortic aneurysm. *Journal of hypertension*, 31(9):1853–60, sep 2013.

[73] Yan Li, Fang-Fei Wei, Shuai Wang, Yi-Bang Cheng, and Ji-Guang Wang. Cardiovascular risks associated with diastolic blood pressure and isolated diastolic hypertension. *Current hypertension reports*, 16(11):489, nov 2014.

[74] M L Lima, A I Fiorelli, D V Vassallo, P R Batista, F V Simoes, J Fiorim, I Stefanon, B B Pinheiro, N A G Stolf, and O M Gomes. Deleterious effect of hypothermia in myocardial protection against cold ischemia: a comparative study in isolated rat hearts. *Transplantation proceedings*, 44(8):2326–32, oct 2012.

[75] Lien-Ying Lin, Yi-Chu Liao, Hsiu-Fen Lin, Yu-Shan Lee, Reuy-Tay Lin, Chung Y Hsu, and Suh-Hang H Juo. Determinants of arterial stiffness progression in a Han-Chinese population in Taiwan: a 4-year longitudinal follow-up. *BMC cardiovascular disorders*, 15(1):100, jan 2015.

[76] Giuseppe Mancia and Guido Grassi. Aggressive Blood Pressure Lowering Is Dangerous: The J-Curve: Pro Side of the Argument. *Hypertension*, 63(1):29–36, nov 2013.

[77] Michael Markl, Wolf Wallis, Christoph Strecker, Beryl Primrose Gladstone, Werner Vach, and Andreas Harloff. Analysis of pulse wave velocity in the thoracic aorta by flow-sensitive four-dimensional MRI: reproducibility and correlation with characteristics in patients with aortic atherosclerosis. *Journal of magnetic resonance imaging : JMRI*, 35(5):1162–8, may 2012.

[78] Susan A Marsh, Louis J Dell'italia, and John C Chatham. Interaction of diet and diabetes on cardiovascular function in rats. *American journal of physiology. Heart and circulatory physiology*, 296(2):H282–92, mar 2009.

[79] Marc W Merx, Cora Schäfer, Ralf Westenfeld, Vincent Brandenburg, Sylvia Hidajat, Christian Weber, Markus Ketteler, and Willi Jahnen-Dechent. Myocardial stiffness, cardiac remodeling, and diastolic dysfunction in calcification-prone fetuin-A-deficient mice. *Journal of the American Society of Nephrology : JASN*, 16(11):3357–64, nov 2005.

[80] G F Mitchell, M A Pfeffer, N Westerhof, and J M Pfeffer. Measurement of aortic input impedance in rats. *The American journal of physiology*, 267(5 Pt 2):H1907–15, nov 1994.

[81] Gary F Mitchell, Marc A Pfeffer, Peter V Finn, and Janice M Pfeffer. Comparison of techniques for measuring pulse-wave velocity in the rat. *Journal of applied physiology (Bethesda, Md. : 1985)*, 82(1):203–10, jan 1997.

[82] William E Moody, Nicola C Edwards, Colin D Chue, Charles J Ferro, and Jonathan N Townend. Arterial disease in chronic kidney disease. *Heart (British Cardiac Society)*, 99(6):365–72, mar 2013.

[83] Eric E Morgan, Andrew B Casabianca, Samer J Khouri, and Andrea L Nestor Kalinoski. In vivo assessment of arterial stiffness in the isoflurane anesthetized spontaneously hypertensive rat. *Cardiovascular ultrasound*, 12:37, jan 2014.

[84] William J Mosley, Philip Greenland, Daniel B Garside, and Donald M Lloyd-Jones. Predictive utility of pulse pressure and other blood pressure measures for cardiovascular outcomes. *Hypertension*, 49(6):1256–64, jun 2007.

[85] Joseph P Murgo, Nico Westerhof, John P Giolma, and Stephen A Altobelli. Aortic input impedance in normal man: relationship to pressure wave forms. *Circulation*, 62(1):105–116, jul 1980.

[86] Wilmer W Nichols. *Cardiac output derived from the aortic pressure*. PhD thesis, Department of Physiology and Biophysics, University of Alabama, 1970.

[87] Wilmer W Nichols and David G Edwards. Arterial Elastance and Wave Reflection Augmentation of Systolic Blood Pressure: Deleterious Effects and Implications for Therapy. *Journal of Cardiovascular Pharmacology and Therapeutics*, 6(1):5–21, mar 2001.

[88] Wilmer W Nichols, Michael F O'Rourke, and Vlachopoulos Charalambos. *McDonald's Blood Flow in Arteries: Theoretical, Experimental and Clinical Principles*. Hodder Arnold, London, 6th edition, 2011.

[89] Nathalie Niederhoffer, Isabelle Lartaud-Idjouadiene, Philippe Giummelly, Claude Duvivier, René Peslin, and Jeffrey Atkinson. Calcification of Medial Elastic Fibers and Aortic Elasticity. *Hypertension*, 29(4):999–1006, apr 1997.

[90] William Noonan, Kristin Koch, Masaki Nakane, Junli Ma, Doug Dixon, Antoinette Bolin, and Glenn Reinhart. Differential effects of vitamin D receptor activators on aortic calcification and pulse wave velocity in uraemic rats. *Nephrology, dialysis, transplantation : official publication of the European Dialysis and Transplant Association - European Renal Association*, 23(12):3824–30, dec 2008.

[91] Michael F O'Rourke. Arterial aging: pathophysiological principles. *Vascular medicine (London, England)*, 12(4):329–41, nov 2007.

[92] Michael F O'Rourke and Junichiro Hashimoto. Mechanical factors in arterial aging: a clinical perspective. *Journal of the American College of Cardiology*, 50(1):1–13, jul 2007.

[93] Michael F O'Rourke, Jan A Staessen, Charalambos Vlachopoulos, Daniel Duprez, and Gérard E Plante. Clinical applications of arterial stiffness; definitions and reference values. *American journal of hypertension*, 15(5):426–44, may 2002.

[94] Anna Paini, Pierre Boutouyrie, David Calvet, Anne-Isabelle Tropeano, Brigitte Laloux, and Stéphane Laurent. Carotid and aortic stiffness: determinants of discrepancies. *Hypertension*, 47(3):371–6, mar 2006.

[95] Subramani Parasuraman and Ramasamy Raveendran. Measurement of invasive blood pressure in rats. *Journal of pharmacology & pharmacotherapeutics*, 3(2):172–7, apr 2012.

[96] Mariëlle M F Poels, Kèren Zaccai, Germaine C Verwoert, Meike W Vernooij, Albert Hofman, Aad van der Lugt, Jacqueline C M Witteman, Monique M B Breteler, Francesco U S Mattace-Raso, and M Arfan Ikram. Arterial stiffness and cerebral small vessel disease: the rotterdam scan study. *Stroke; a journal of cerebral circulation*, 43(10):2637–42, oct 2012.

[97] J D Pruett, J D Bourland, and L A Geddes. Measurement of pulse-wave velocity using a beat-sampling technique. *Annals of biomedical engineering*, 16(4):341–7, jan 1988.

[98] Ahmed Qasem and Alberto Avolio. Determination of aortic pulse wave velocity from waveform decomposition of the central aortic pressure pulse. *Hypertension*, 51(2):188–95, feb 2008.

[99] Karen Quirk and Dennis F Bandyk. Interpretation of carotid duplex testing. *Seminars in vascular surgery*, 26(2-3):72–85, jan 2013.

[100] R Core Team. *R: A Language and Environment for Statistical Computing*. R Foundation for Statistical Computing, Vienna, Austria, 2014.

[101] S W Rabkin and A Y Fung. Increased sensitivity to norepinephrine cardiac arrhythmias in the deoxycorticosterone acetate high salt rat before the onset of hypertension. *Canadian journal of physiology and pharmacology*, 62(6):605–9, jun 1984.

[102] Noel Rappin and Robin Dunn. wxPython in Action. mar 2006.

[103] James C Russell and Spencer D Proctor. Small animal models of cardiovascular disease: tools for the study of the roles of metabolic syndrome, dyslipidemia, and atherosclerosis. *Cardiovascular pathology : the official journal of the Society for Cardiovascular Pathology*, 15(6):318–30, jan 2006.

[104] Gale H Rutan, Robert H McDonald, and Lewis H Kuller. A historical perspective of elevated systolic vs diastolic blood pressure from an epidemiological and clinical trial viewpoint. *Journal of clinical epidemiology*, 42(7):663–73, jan 1989.

[105] Sangeetha Satheesan, J L Figarola, T Dabbs, S Rahbar, and R Ermel. Effects of a new advanced glycation inhibitor, LR-90, on mitigating arterial stiffening and improving arterial elasticity and compliance in a diabetic rat model: aortic impedance analysis. *British journal of pharmacology*, 171(12):3103–14, jun 2014.

[106] Patrick Segers, Ernst R Rietzschel, Marc L De Buyzere, Dirk De Bacquer, Luc M Van Bortel, Guy De Backer, Thierry C Gillebert, and Pascal R Verdonck. Assessment of pressure wave reflection: getting the timing right! *Physiological measurement*, 28(9):1045–56, sep 2007.

[107] Robert E Shadwick. Mechanical design in arteries. *J. Exp. Biol.*, 202(23):3305–3313, dec 1999.

[108] James E Sharman, Thomas H Marwick, Deborah Gilroy, Petr Otahal, Walter P Abhayaratna, and Michael Stowasser. Randomized trial of guiding hypertension management using central aortic blood pressure compared with best-practice care: principal findings of the BP GUIDE study. *Hypertension*, 62(6):1138–45, dec 2013.

[109] Dave Shreiner and The Khronos OpenGL ARB Working Group. OpenGL Programming Guide: The Official Guide to Learning OpenGL, Versions 3.0 and 3.1. jul 2009.

[110] P Sobolewski and M El Fray. Cardiac catheterization: consequences for the endothelium and potential for nanomedicine. *Wiley interdisciplinary reviews. Nanomedicine and nanobiotechnology*, 7(3):458–73.

[111] E Brooke Spencer, Douglas H Sheafor, Barbara S Hertzberg, James D Bowie, Rendon C Nelson, Barbara A Carroll, and Mark A Kliewer. Nonstenotic internal carotid arteries: effects of age and blood pressure at the time of scanning on Doppler US velocity measurements. *Radiology*, 220(1):174–8, jul 2001.

[112] Jan A Staessen, Jerzy Gasowski, Ji G Wang, Lutgarde Thijs, Elly Den Hond, Jean-Pierre Boissel, John Coope, Tork Ekbom, François Gueyffier, Lisheng Liu, Karla Kerlikowske, Stuart Pocock, and Robert H Fagard. Risks of untreated and treated isolated systolic hypertension in the elderly: meta-analysis of outcome trials. *Lancet (London, England)*, 355(9207):865–72, mar 2000.

[113] Jan A Staessen, Ji-Guang Wang, and Lutgarde Thijs. Cardiovascular protection and blood pressure reduction: a meta-analysis. *The Lancet*, 358(9290):1305–1315, oct 2001.

[114] Jun Sugawara, Hidehiko Komine, Koichiro Hayashi, Seiji Maeda, and Mitsuo Matsuda. Relationship between augmentation index obtained from carotid and radial artery pressure waveforms. *Journal of hypertension*, 25(2):375–81, feb 2007.

[115] Isabella Tan, Mark Butlin, Ying Yi Liu, Keith Ng, and Alberto P Avolio. Heart rate dependence of aortic pulse wave velocity at different arterial pressures in rats. *Hypertension*, 60(2):528–33, aug 2012.

[116] Jean-Michel Tartière, Jean-Yves Tabet, Damien Logeart, Lamia Tartière-Kesri, Florence Beauvais, Christophe Chavelas, and Alain Cohen Solal. Noninvasively determined radial dP/dt is a predictor of mortality in patients with heart failure. *American heart journal*, 155(4):758–63, apr 2008.

[117] Michael G Taylor. An Approach to an Analysis of the Arterial Pulse Wave I. Oscillations in an Attenuating Line. *Physics in Medicine and Biology*, 1(3):258–269, jan 1957.

[118] Michael G Taylor. An Approach to an Analysis of the Arterial Pulse Wave II. Fluid Oscillations in an Elastic Pipe. *Physics in Medicine and Biology*, 1(4):321–329, apr 1957.

[119] M Tjepkema, R Wilkins, N Goedhuis, and J Pennock. Cardiovascular disease mortality among First Nations people in Canada, 1991-2001. *Chronic diseases and injuries in Canada*, 32(4):200–7, sep 2012.

[120] Vitor E Valenti, Luiz Carlos de Abreu, Hugo Macedo Junior, Oseas F Moura Filho, and Celso Ferreira. Baroreflex sensitivity differs among same strain Wistar rats from the same laboratory. *Heart international*, 6(2):e9, jan 2011.

[121] Nicole M van Popele, Diederick E Grobbee, Michiel L Bots, Roland Asmar, Jirar Topouchian, Robert S Reneman, Arnold P G Hoeks, Deidre A M van der Kuip, Albert Hofman, and Jacqueline C M Witteman. Association Between Arterial Stiffness and Atherosclerosis : The Rotterdam Study. *Stroke*, 32(2):454–460, feb 2001.

[122] Guido Van Rossum and Fred L Drake Jr. *Python reference manual*. Centrum voor Wiskunde en Informatica Amsterdam, 1995.

[123] Thomas T van Sloten, Miranda T Schram, Katja van den Hurk, Jacqueline M Dekker, Giel Nijpels, Ronald M A Henry, and Coen D A Stehouwer. Local stiffness of the carotid and femoral artery is associated with incident cardiovascular events and all-cause mortality: the Hoorn study. *Journal of the American College of Cardiology*, 63(17):1739–47, may 2014.

[124] Paolo Verdecchia, Fabio Angeli, Giovanni Mazzotta, Marta Garofoli, and Gianpaolo Reboldi. Aggressive Blood Pressure Lowering Is Dangerous: The J-Curve: Con Side of the Argument. *Hypertension*, 63(1):37–40, nov 2013.

[125] Charalambos Vlachopoulos, Konstantinos Aznaouridis, Michael F O'Rourke, Michel E Safar, Katerina Baou, and Christodoulos Stefanadis. Prediction of cardiovascular events and all-cause mortality with central haemodynamics: a systematic review and meta-analysis. *European heart journal*, 31(15):1865–71, aug 2010.

[126] Charalambos Vlachopoulos, Konstantinos Aznaouridis, and Christodoulos Stefanadis. Prediction of cardiovascular events and all-cause mortality with arterial stiffness: a systematic review and meta-analysis. *Journal of the American College of Cardiology*, 55(13):1318–27, mar 2010.

[127] Charalambos Vlachopoulos, Panagiotis Xaplanteris, Victor Aboyans, Marianne Brodmann, Renata Cífková, Francesco Cosentino, Marco De Carlo, Augusto Gallino, Ulf Landmesser, Stéphane Laurent, John Lekakis, Dimitri P Mikhailidis, Katerina K Naka, Athanasios D Protogerou, Damiano Rizzoni, Arno Schmidt-Trucksäss, Luc Van Bortel, Thomas Weber, Akira Yamashina, Reuven Zimlichman, Pierre Boutouyrie, John Cockcroft, Michael O'Rourke, Jeong Bae Park, Giuseppe Schillaci, Henrik Sillesen, and Raymond R Townsend. The role of vascular biomarkers for primary and secondary prevention. A position paper from the European Society of Cardiology Working Group on peripheral circulation: Endorsed by the Association for Research into Arterial Structure and Physiology (ARTERY. *Atherosclerosis*, 241(2):507–32, aug 2015.

[128] Kang-Ling Wang, Hao-Min Cheng, Shih-Hsien Sung, Shao-Yuan Chuang, Cheng-Hung Li, Harold A Spurgeon, Chih-Tai Ting, Samer S Najjar, Edward G Lakatta, Frank C P Yin, Pesus Chou, and Chen-Huan Chen. Wave reflection and arterial stiffness in the prediction of 15-year all-cause and cardiovascular mortalities: a community-based study. *Hypertension*, 55(3):799–805, mar 2010.

[129] Y Wang, J N Yang, A Arner, P J M Boels, and B B Fredholm. Adenosine A(1) receptors and vascular reactivity. *Acta physiologica (Oxford, England)*, 199(2):211–20, jun 2010.

[130] Thomas Weber, Siegfried Wassertheurer, Martin Rammer, Anton Haiden, Bernhard Hametner, and Bernd Eber. Wave reflections, assessed with a novel method for pulse wave separation, are associated with end-organ damage and clinical outcomes. *Hypertension*, 60(2):534–41, aug 2012.

[131] Thomas Weber, Siegfried Wassertheurer, Martin Rammer, Anton Haiden, Bernhard Hametner, and Bernd Eber. Wave reflections, assessed with a novel method for pulse

wave separation, are associated with end-organ damage and clinical outcomes. *Hypertension*, 60(2):534–41, aug 2012.

[132] Berend E Westerhof, Ilja Guelen, Nico Westerhof, John M Karemaker, and Alberto Avolio. Quantification of wave reflection in the human aorta from pressure alone: a proof of principle. *Hypertension*, 48(4):595–601, oct 2006.

[133] N Westerhof, P Sipkema, G C van den Bos, and G Elzinga. Forward and backward waves in the arterial system. *Cardiovascular research*, 6(6):648–56, nov 1972.

[134] Nico Westerhof and P Sipkema. Measurement of pulse wave velocity using a beat-sampling technique. *Annals of biomedical engineering*, 17(3):309–11, jan 1989.

[135] Nico Westerhof, Nikos Stergiopulos, and Mark I.M. Noble. *Snapshots of Hemodynamics*, volume 18 of *Basic Science for the Cardiologist*. Kluwer Academic Publishers, Boston, 2005.

[136] Seamus P Whelton, Ron Blankstein, Mouaz H Al-Mallah, Joao A C Lima, David A Bluemke, W Gregory Hundley, Joseph F Polak, Roger S Blumenthal, Khurram Nasir, and Michael J Blaha. Association of resting heart rate with carotid and aortic arterial stiffness: multi-ethnic study of atherosclerosis. *Hypertension*, 62(3):477–84, sep 2013.

[137] Wenxin Xu, Saveli I Goldberg, Maria Shubina, and Alexander Turchin. Optimal systolic blood pressure target, time to intensification, and time to follow-up in treatment of hypertension: population based retrospective cohort study. *BMJ (Clinical research ed.)*, 350:h158, jan 2015.

[138] Jieyun You, Jian Wu, Junbo Ge, and Yunzeng Zou. Comparison between adenosine and isoflurane for assessing the coronary flow reserve in mouse models of left ventricular pressure and volume overload. *American journal of physiology. Heart and circulatory physiology*, 303(10):199–207, sep 2012.

[139] Susan J Zieman, Vojtech Melenovsky, and David A Kass. Mechanisms, pathophysiology, and therapy of arterial stiffness. *Arteriosclerosis, thrombosis, and vascular biology*, 25(5):932–43, may 2005.

[140] Armin Zittermann, Stefanie S Schleithoff, and Reiner Koerfer. Vitamin D and vascular calcification. *Current opinion in lipidology*, 18(1):41–6, feb 2007.

Appendix A

Representing the arterial system as a transmission line

A transmission line is an electrical circuit component that is designed to carry high frequency alternating current. Wave separation analysis, WSA, is based on modeling the arterial system as a transmission line carrying an alternating current. Figure A.1 shows the simplest example of a transmission line that consists of two wires of infinite length running in parallel as part of a larger circuit that carries alternating current. The behavior of the transmission line in Figure A.1 can be described by a single real parameter called characteristic impedance Z_c assuming the wires are uniform, have no loss of power, and are of infinite length. If there are discontinuities in the transmission line, the alternating current is reflected back to the source.

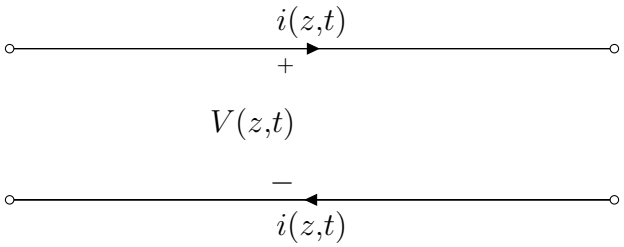

Figure A.1: A simple linear transmission line represented as two wires of infinite length. At a distance z along the wire from some origin, there is an alternating current sinusoidal wave of $i(z,t)$ travelling through each wire, and this creates a voltage difference of $V(z,t)$. With a single wave traveling through the wire and no reflections produced at the end of the transmission line, the system is decribed by the characteristic impedance $Z_c = V(z,t)/i(z,t)$. The characteristic impedance is purely real and does not depend on z in a uniform wire that is lossless.

The transmission line model describing a segment of artery is shown in Figure A.2. The inductor L resists changes in electrical current passing through it. The resistor R reduces the current and voltage levels in the circuit. The capacitor C stores energy in an electrostatic field between its plates. The telegraph equations describing the transmission line model of the arterial system are given by Equations A.1 and A.2.

$$-\frac{\partial V}{\partial z} = L'\frac{\partial i}{\partial t} + R'i, \tag{A.1}$$

$$-\frac{\partial i}{\partial z} = C'\frac{\partial V}{\partial t} + \frac{V}{R'_l}, \tag{A.2}$$

where z is distance, t is time, $V = V(z,t)$ is voltage, L' is inductance per unit length, C' is capacitance per unit length, $i = i(z,t)$ is current, R' resistance per unit length, and $\frac{1}{R'_l}$ is the leakage per length [50].

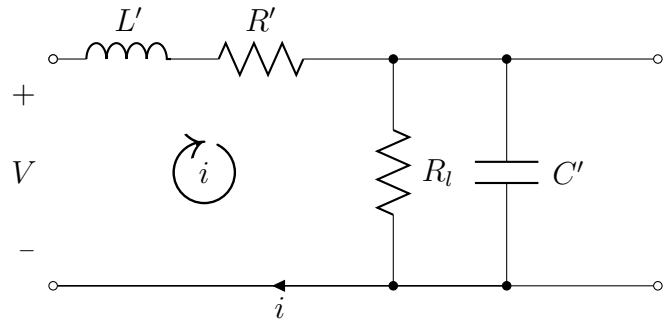

Figure A.2: Transmission model of an arterial segment of length δz. L' is inductance per length, C' is capacitance per length, $i \triangleq i(z,t)$ is current, R' resistance per length, $R_l \triangleq \frac{R'_l}{\delta z}$ where $\frac{1}{R'_l}$ is the conductance per unit length, and $V \triangleq V(z,t)$ is voltage [50].

The linearized Navier Stokes equations that describe the blood flow, Q, and pressure, P, in a short segment of artery with a constant cross-sectional area and homogeneous and isotropic wall material are as follows:

$$-\frac{\partial P}{\partial z} = \frac{\rho}{S}\frac{\partial Q}{\partial t} + WQ \tag{A.3}$$

$$-\frac{\partial Q}{\partial z} = \frac{\partial S}{\partial P}\frac{\partial P}{\partial t} + Gp \tag{A.4}$$

where $P = P(z,t)$ is pressure, z is the position, S is the cross-sectional area, ρ is the density of blood, $\frac{\rho}{S}$ is the inertia per unit length, $Q = Q(x,t)$ is flow, t is time, W is friction per unit length, G is the leakage per unit length, and $\frac{\partial S}{\partial P}$ is the distensibility per unit length.

The telegraph equations are mathematically equivalent to the linearized Navier Stokes equations via the associations of flow with current, pressure with voltage, inertia with inductance, friction with resistance, distensibility with capacitance, and leakage G with $\frac{1}{R'_l}$ [50].

Appendix B

Fourier Analysis

The coefficients a_0, a_n, and b_n, $n \in \mathbb{Z}^+$ for the Fourier series harmonics of angular frequency w are computed for a single waveform $g(x)$:

$$g(x) = a_0 + \sum_{n=1}^{\infty} a_n \cos(n\omega x) + \sum_{n=1}^{\infty} b_n \sin(n\omega x), \tag{B.1}$$

where $w = 2\pi f$, $f = \frac{1}{t_2 - t_1}$, t_1 is the beginning of a cardiac cycle, and t_2 is the end of the same cardiac cycle. Note that $t_2 - t_1$ corresponds to the period of the cardiac cycle. Equation B.1 can be solved for a_0 when multiplied by 1, which is the basis function for a_0, and integrated over the domain t_1 to t_2,

$$\int_{t_1}^{t_2} g(x)dx = a_0 \int_{t_1}^{t_2} 1dx + \sum_{n=1}^{\infty} a_n \int_{t_1}^{t_2} \cos(n\omega x)dx + \sum_{n=1}^{\infty} b_n \int_{t_1}^{t_2} \sin(n\omega x)dx.$$

The trignometric integrals over the domain t_1 to t_2 are:

$$\int_{t_1}^{t_2} \cos(n\omega x)dx = 0,$$

$$\int_{t_1}^{t_2} \sin(n\omega x)dx = 0,$$

and the coefficient a_0 can be solved for:

$$a_0 = \frac{\int_{t_1}^{t_2} g(x)dx}{(t_2 - t_1)}. \tag{B.2}$$

Equation B.1 can be solved for a_m for an arbitrary $m \in \mathbb{Z}^+$ by multiplying both sides of equation B.1 by the basis function $\cos(m\omega x)$,

$$\int_{t_1}^{t_2} g(x)\cos(m\omega x)dx = a_0 \int_{t_1}^{t_2} \cos(m\omega x)dx + \sum_{n=1}^{\infty} a_n \int_{t_1}^{t_2} \cos(n\omega x)\cos(m\omega x)dx$$
$$+ \sum_{n=1}^{\infty} b_n \int_{t_1}^{t_2} \sin(n\omega x)\cos(m\omega x)dx.$$

The trigonometric integrals over the domain t_1 to t_2 are:

$$\int_{t_1}^{t_2} \cos(m\omega x)dx = 0,$$

$$\int_{t_1}^{t_2} \cos(n\omega x)\cos(m\omega x)dx = 0 \quad \text{when } n \neq m,$$

$$\int_{t_1}^{t_2} \cos(n\omega x)\cos(m\omega x)dx = \int_{t_1}^{t_2} \cos^2(m\omega x)dx = \frac{t_2 - t_1}{2} \quad \text{when } n = m,$$

$$\int_{t_1}^{t_2} \sin(n\omega x)\cos(m\omega x)dx = 0.$$

The coefficient a_m can then be solved for:

$$a_m = \frac{2\int_{t_1}^{t_2} g(x)\cos(m\omega x)dx}{t_2 - t_1}. \tag{B.3}$$

Equation B.1 can be solved for b_m for an arbitrary $m \in \mathbb{Z}^+$ by multiplying both sides of equation B.1 by the basis function $\sin(m\omega x)$,

$$\int_{t_1}^{t_2} g(x)\sin(m\omega x)dx = a_0 \int_{t_1}^{t_2} \sin(m\omega x)dx + \sum_{n=1}^{\infty} a_n \int_{t_1}^{t_2} \cos(n\omega x)\sin(m\omega x)dx$$
$$+ \sum_{n=1}^{\infty} b_n \int_{t_1}^{t_2} \sin(n\omega x)\sin(m\omega x)dx.$$

The trigonometric integrals over the domain t_1 to t_2 are:

$$\int_{t_1}^{t_2} \sin(m\omega x)dx = 0,$$

$$\int_{t_1}^{t_2} \cos(n\omega x)\sin(m\omega x)dx = 0$$

$$\int_{t_1}^{t_2} \sin(n\omega x)\sin(m\omega x)dx = 0 \quad \text{when } n \neq m,$$

$$\int_{t_1}^{t_2} \sin(n\omega x)\sin(m\omega x)dx = \int_{t_1}^{t_2} \sin^2(m\omega x)dx = \frac{t_2 - t_1}{2} \quad \text{when } n = m.$$

The coefficients b_m can then be solved for:

$$b_m = \frac{2\int_{t_1}^{t_2} g(x)\sin(m\omega x)dx}{t_2 - t_1}. \tag{B.4}$$

Using trignometric identities, the coefficients can be converted into the phase angle form that is traditionally used for wave separation analysis [88]:

$$\begin{aligned} g(x) &= a_0 + \sum_{n=1}^{\infty} c_n \cos(n\omega x + \varphi_n), \\ c_n &= \sqrt{a_n^2 + b_n^2}, \\ \varphi_n &= \arctan\left(-\frac{b_n}{a_n}\right), \end{aligned}$$

where c_n is the amplitude and φ_n is the phase angle.

Appendix C

Phasor Arithmetic

The phase angle form of the Fourier Series can be transformed into a phasor that is represented as a complex number.

$$|M_n| \cos(\omega n t + \varphi_n) = \mathrm{Re}\left\{|M_n| \, e^{i(\omega n t + \varphi)}\right\}$$

where n is a particular harmonic of the fourier series, M_n is the modulus of the fourier series nth harmonic, ω is the angular frequency, andφ_n is the phase shift of the fourier series nth harmonic.

The phasor form is simplified for addition, subtraction, multiplication, and division of sinusoids with the same angular frequency, ω, and harmonic, n. Once simplified, the phasors can be expressed in exponential phasor form (equation C.1), in rectangular phasor form (equation C.2), and in phasor notation (equation C.3).

$$z = |M| \, e^{i\varphi} \tag{C.1}$$
$$= A + iB \tag{C.2}$$
$$= |M|_{\angle\varphi} \tag{C.3}$$

Multiplication of two phasors involves multiplying their moduli and adding together their phases (equation C.4). Division of two phasors involves dividing their moduli and subtracting their phases (equation C.5).

$$z_1 = M_{1\angle\varphi_1}$$
$$z_2 = M_{2\angle\varphi_2}$$
$$z_1 \times z_2 = M_1 \times M_{2\angle\varphi_1+\varphi_2} \tag{C.4}$$
$$\frac{z_1}{z_2} = \frac{M_1}{M_2}_{\angle\varphi_1-\varphi_2} \tag{C.5}$$

Addition (Equation C.6) and subtraction (Equation C.7) of phasors occurs after being converted into rectangular form.

$$A = |M| \cos(\varphi)$$
$$B = |M| \sin(\varphi)$$
$$z_1 = A_1 + iB_1$$
$$z_2 = A_2 + iB_2$$
$$z_1 + z_2 = (A_1 + A_2) + i(B_1 + B_2) \tag{C.6}$$
$$z_1 - z_2 = (A_1 - A_2) + i(B_1 - B_2) \tag{C.7}$$

The rectangular form can be converted back into exponential form by:

$$M = \sqrt{A^2 + B^2},$$
$$\varphi = \arctan(\frac{B}{A}).$$